

1  
2 **RESEARCH ARTICLE**

3  
4 **Abscisic Acid-Triggered Persulfidation of the Cysteine Protease ATG4**  
5 **Mediates Regulation of Autophagy by Sulfide**

6  
7 Ana M. Laureano-Marín<sup>a,1</sup>, Ángeles Aroca<sup>a,1</sup>, M. Esther Pérez-Pérez<sup>a</sup>, Inmaculada  
8 Yruela<sup>b,c</sup>, Ana Jurado-Flores<sup>a</sup>, Inmaculada Moreno<sup>a</sup>, José L. Crespo<sup>a</sup>, Luis C. Romero<sup>a</sup>,  
9 Cecilia Gotor<sup>a,2</sup>

10  
11 <sup>a</sup>Instituto de Bioquímica Vegetal y Fotosíntesis, Consejo Superior de Investigaciones Científicas  
12 and Universidad de Sevilla, Seville, Spain

13 <sup>b</sup>Estación Experimental de Aula Dei, Consejo Superior de Investigaciones Científicas,  
14 Zaragoza, Spain

15 <sup>c</sup>Group of Biochemistry, Biophysics and Computational Biology (BIFI-Unizar) Joint Unit to  
16 CSIC, Spain

17  
18 <sup>1</sup>These authors contributed equally to this work

19 <sup>2</sup>Address correspondence to [gotor@ibvf.csic.es](mailto:gotor@ibvf.csic.es).

20  
21 **Short title:** ATG4 is a target of sulfide

22  
23 **One-sentence summary:** Hydrogen sulfide negatively regulates the progress of autophagy  
24 through persulfide modification of the Arabidopsis AtATG4a protease

25  
26 The author responsible for distribution of materials integral to the findings presented in this  
27 article in accordance with the policy described in the Instructions for Authors  
28 ([www.plantcell.org](http://www.plantcell.org)) is: Cecilia Gotor ([gotor@ibvf.csic.es](mailto:gotor@ibvf.csic.es)).

29  
30  
31 **ABSTRACT**

32  
33 Hydrogen sulfide is a signaling molecule that regulates essential processes in plants,  
34 such as autophagy. In *Arabidopsis thaliana*, hydrogen sulfide negatively regulates  
35 autophagy independently of reactive oxygen species via an unknown mechanism.  
36 Comparative and quantitative proteomic analysis was used to detect abscisic acid-  
37 triggered persulfidation that reveals a main role in the control of autophagy mediated by  
38 the autophagy-related (ATG) cysteine protease AtATG4a. This protease undergoes  
39 specific persulfidation of Cys170 that is a part of the characteristic catalytic Cys-His-  
40 Asp triad of cysteine proteases. Regulation of the ATG4 activity by persulfidation was  
41 tested in a heterologous assay using the *Chlamydomonas reinhardtii* CrATG8 protein as  
42 a substrate. Sulfide significantly and reversibly inactivates AtATG4a. The biological  
43 significance of the reversible inhibition of the ATG4 by sulfide is supported by the  
44 results obtained in Arabidopsis leaves under basal and autophagy-activating conditions.  
45 A significant increase in the overall ATG4 proteolytic activity in Arabidopsis was

46 detected under nitrogen starvation and osmotic stress and can be inhibited by sulfide.  
47 Therefore, the data strongly suggest that the negative regulation of autophagy by sulfide  
48 is mediated by specific persulfidation of the ATG4 protease.

49

50

## 51 **INTRODUCTION**

52

53 Hydrogen sulfide is currently recognized as a signaling molecule. In plant systems, H<sub>2</sub>S  
54 is considered to be as important as NO and H<sub>2</sub>O<sub>2</sub> and regulates essential processes of  
55 plant performance (Garcia-Mata and Lamattina, 2013; Calderwood and Kopriva, 2014;  
56 Jin and Pei, 2015; Gotor et al., 2017). Sulfide mediates tolerance against a range of  
57 plant stresses from heavy metal toxicity to salinity and drought to enhance plant  
58 viability (Gotor et al., 2019). Sulfide regulates critical processes, including autophagy  
59 (Alvarez et al., 2012; Gotor et al., 2013; Gotor et al., 2015; Laureano-Marin et al.,  
60 2016b; Laureano-Marin et al., 2016a) and the abscisic acid (ABA)-dependent stomatal  
61 movement (Jin et al., 2013; Scuffi et al., 2014; Papanatsiou et al., 2015; Scuffi et al.,  
62 2018).

63 Despite increasing evidence of the biological function of H<sub>2</sub>S, there is a considerable  
64 lack of information on the mechanism of action of H<sub>2</sub>S in particular physiological  
65 processes. The mechanism of action must be related to chemical reactivity of H<sub>2</sub>S with  
66 other molecules. H<sub>2</sub>S was suggested to coordinate the metal centers of metalloproteins  
67 (Vitvitsky et al., 2018) or act as a reductant of reactive oxygen species (Zaffagnini et al.,  
68 2019). A third mechanism of action of H<sub>2</sub>S is based on its ability to modify the thiol  
69 group (-SH) of the cysteine residues in target proteins to form a persulfide group (-SSH)  
70 resulting in functional changes in the protein structure, activity, or subcellular  
71 localizations (Aroca et al., 2015; Aroca et al., 2017b). This posttranslational  
72 modification is called persulfidation (known previously as S-sulfhydration) and has  
73 been initially demonstrated in the mammalian (Mustafa et al., 2009; Paul and Snyder,  
74 2012) and plant systems (Aroca et al., 2015; Aroca et al., 2017a) using specific labeling  
75 methods.

76 Our previous investigations in *Arabidopsis thaliana* demonstrated that hydrogen  
77 sulfide functions as a signaling molecule in the cytosol that negatively regulates  
78 autophagy (Alvarez et al., 2012; Gotor et al., 2013; Romero et al., 2013), which is a  
79 highly conserved process involving digestion of the cell contents for recycling and

80 maintenance of cell homeostasis. Autophagy occurs at the basal levels in eukaryotic  
81 cells and is induced by internal or external perturbations. In plants, autophagy is  
82 involved in development, immune response, and senescence and is induced by stress  
83 conditions, including nutrient limitation and other abiotic stresses (Liu and Bassham,  
84 2012; Pérez-Pérez et al., 2012; Masclaux-Daubresse et al., 2017; Ustun et al., 2017;  
85 Marshall and Vierstra, 2018a). This catabolic process is characterized by *de novo*  
86 synthesis of autophagosomes in the cytosol, in which cytoplasmic materials to be  
87 recycled are sequestered, transported, and released into the plant vacuole. Various  
88 receptors have been described to assist with specific cargo recruitment and degradation  
89 via selective autophagy. The core autophagy machinery is highly conserved in all  
90 studied eukaryotes, and involved proteins are referred to as autophagy-related (ATG).  
91 These ATG proteins include the ATG8 and ATG12 ubiquitin-like conjugation systems  
92 that catalyze the covalent attachment of ATG8 to the phospholipid  
93 phosphatidylethanolamine (PE), which is an essential adduct for the formation of  
94 autophagosomes (Mizushima et al., 2011). Before this conjugation, the C-terminal  
95 extension of newly synthesized ATG8 has to be cleaved by the Cys-type protease ATG4  
96 to expose a highly conserved Gly, which is necessary for conjugation to PE.  
97 Additionally, ATG4 functions as a deconjugating enzyme that cleaves the amide bond  
98 between ATG8 and PE allowing the recycling of free ATG8 (Nair et al., 2012;  
99 Nakatogawa et al., 2012; Yu et al., 2012).

100 The role of sulfide as a repressor of autophagy is independent of nutrient conditions  
101 and specific tissues because sulfide inhibits autophagy in leaves under dark-induced  
102 carbon starvation (Alvarez et al., 2012) or in roots under nitrogen deprivation  
103 (Laureano-Marin et al., 2016a), and both conditions are unrelated to sulfur metabolism.  
104 A study aiming to decipher the mechanism of action of H<sub>2</sub>S showed that it is  
105 independent of the formation of reactive oxygen species (ROS), such as hydrogen  
106 peroxide or superoxide anions, and therefore H<sub>2</sub>S does not serve as a reducer in the  
107 regulation of autophagy (Laureano-Marin et al., 2016a). Interestingly, a comparative  
108 and quantitative proteomic analysis was performed to detect endogenous persulfidated  
109 proteins; the results indicated that at least 10% of the entire Arabidopsis proteome  
110 undergoes persulfidation under physiological conditions suggesting a widespread  
111 distribution of this posttranslational modification (Aroca et al., 2017a). Furthermore,  
112 persulfidation of various components of the ABA signaling pathway has been recently

113 described as a specific mechanism of action by which H<sub>2</sub>S controls the guard cell ABA  
114 signaling (Chen et al., 2020; Shen et al., 2020).

115 In this study, a comparative and quantitative proteomic analysis was used to detect  
116 persulfidated proteins in the leaves of Arabidopsis exogenously treated with ABA.  
117 Interestingly, comparison of the untreated and ABA-treated samples indicated that  
118 AtATG4a was the protein with the highest difference in the persulfidation level. We  
119 then sought to determine whether persulfidation is the mechanism of the regulation of  
120 autophagy by sulfide in Arabidopsis under the stress conditions and to ascertain whether  
121 persulfidation regulates the activity of ATG4. To this aim, an enzymatic assay using  
122 *Chlamydomonas reinhardtii* CrATG8 as ATG4 substrate was developed. In-depth  
123 analysis of ATG4 proteolytic activity was performed *in vitro* and in a cell-free system  
124 using total extracts from Arabidopsis under basal or autophagy-activating conditions,  
125 including nitrogen limitation or osmotic stress. The results indicate that ATG4 is a  
126 specific target of persulfidation.

127  
128

## 129 **RESULTS**

130

### 131 **Autophagy induction by abscisic acid-triggered persulfide modification is** 132 **mediated by AtATG4a regulation by hydrogen sulfide in Arabidopsis**

133

134 Abscisic acid can trigger changes in hydrogen sulfide level and protein persulfide  
135 modification in the guard cells to modulate stomatal closure (Shen et al., 2020). To  
136 assess whether ABA also regulates protein persulfidation levels in the mesophyll cells, a  
137 sequential window acquisition of all theoretical spectra-mass spectrometry (SWATH-  
138 MS) quantitative approach was combined with the tag-switch method to measure  
139 protein persulfidation (Aroca et al., 2017a). Protein samples from three biological  
140 replicates (independent pools) of leaf tissue treated with ABA for 0 h (control sample),  
141 3 h, and 6 h were isolated and subjected to the tag-switch procedure (Figure 1A). The  
142 proteins eluted from the streptavidin beads were digested, and the peptide solutions  
143 analyzed in two sequential steps: a shotgun data-dependent acquisition (DDA) approach  
144 to generate the spectral library and SWATH acquisition by the data-independent  
145 acquisition (DIA) method. In the first step, integration of the nine datasets resulted in  
146 identification of a total of 10,329 peptides (1% FDR and 90% confidence) and 1,434

147 unique proteins (1% FDR) that were used as a spectral library (Supplemental Dataset 1).  
148 In the second step, to quantify protein levels using SWATH acquisition, the same six  
149 biological samples were analyzed in two technical replicates by the DIA method using  
150 the LC gradient and LC-MS equipment employed in generation of the spectral library.

151 Therefore, six datasets were generated from the control and ABA-treated (for 3 and 6  
152 h) samples to yield a total of 18 datasets used for the quantitative analysis. The fragment  
153 spectra were extracted for the eighteen runs, and 33,887 ion transitions, 4,871 peptides,  
154 and 1,157 proteins were quantified. Principal component analysis (PCA) of the protein  
155 sample subgroups revealed significant reproducible data between the replicates and  
156 differences between the ABA treatments (Figure 1B).

157 Comparison between the control (0 h) and the 3 h ABA treatment samples (0 h vs 3 h  
158 ABA; Supplemental Dataset 2) showed that 192 proteins were more abundant in the  
159 control samples with the fold change  $> 1.5$  ( $p$  value  $< 0.05$ ), and 242 proteins were less  
160 abundant with the fold change  $< 0.66$  ( $p$  value  $< 0.05$ ) (Supplemental Dataset 3) (Figure  
161 1C). Higher abundance of a protein in the control samples than that in the samples  
162 prepared after 3 h ABA treatment means that the protein is more persulfidated in the  
163 control because the tag-switch labeling recovers more protein from the streptavidin  
164 column. Lower abundance in the control means that a protein is more persulfidated in  
165 the 3 h ABA samples.

166 A total of 192 proteins with reduced persulfidation level after 3 h of ABA treatment  
167 were analyzed based on their assigned functions and classified into 32 functional groups  
168 using the MapMan nomenclature (Thimm et al., 2004; Klie and Nikoloski, 2012)  
169 (Supplemental Table 1). The most numerous set corresponded to the general protein  
170 group (bin 29) (Supplemental Table 2), which included 18.2% of the total identified  
171 proteins with 35 total elements, 29 of which are involved in protein amino acid  
172 activation (8 elements, tRNA ligases), protein synthesis (12 elements) and protein  
173 degradation (9 elements). The latter group included the Cys-type protease AtATG4a  
174 involved in autophagy, which showed the highest persulfidation change (5.20-fold  
175 change), and the S1 RNA-BINDING RIBOSOMAL PROTEIN 1 (3.69-fold change)  
176 that regulates seedling growth in the presence ABA or under abiotic stress conditions  
177 (Gu et al., 2015). Additional proteins involved in the regulatory process and with a  
178 reduction in their persulfidation levels included MAPK kinase 6 (MPK6, AT2G43790),  
179 tyrosine phosphatase 1 (PTP1, AT1G71860), glycine-rich protein 8 (GRP8,  
180 AT4G39260), and 9-cis-epoxycarotenoid dioxygenase 4 (NCED4, AT4G19170).

181 The quantitative analysis of the control and the 6 h ABA treatment samples  
182 (Supplemental Dataset 4) showed a reduction in the number of regulated proteins; only  
183 120 proteins were more abundant in the control *versus* the ABA treatment samples with  
184 the fold change > 1.5 ( $p$  value < 0.05), and 198 proteins were less abundant with the  
185 fold change < 0.66 ( $p$  value < 0.05) (Supplemental Dataset 5) (Figure 1C).

186 Comparison of differentially regulated proteins at 3 and 6 h of ABA treatment  
187 showed that 42% of the proteins are regulated under both conditions and had different  
188 levels of persulfidation. The cysteine protease AtATG4a showed a reduction in the level  
189 of persulfidation down to only 2.45-fold after 6 h of ABA treatment compared to that  
190 under the control conditions; this level was higher than that in the 3 h ABA treatment  
191 samples (Figure 1D). Therefore, persulfidation level of AtATG4a was transiently  
192 reduced after a short ABA treatment, and this reduction was very significant compared  
193 to the untreated control.

194 The proteomics data suggest that AtATG4a protease is differentially persulfidated  
195 depending on the treatment conditions; this difference may be related to the progress of  
196 autophagy. To test this assumption, we analyzed the regulation of autophagy by ABA  
197 treatments and the effects of sulfide under these conditions. Arabidopsis seedlings  
198 expressing GFP-ATG8e fusion protein (Xiong et al., 2007) were treated with 50  $\mu$ M  
199 ABA for 3 and 6 h and subjected to additional treatment of 200  $\mu$ M NaHS for 1 h. Total  
200 protein extracts were obtained, and immunoblot analysis was performed using anti-GFP  
201 antibodies to detect free GFP and the GFP-ATG8e fusion protein (Figure 2A). A clear  
202 increase in the free GFP protein level in ABA-treated seedlings was detected compared  
203 with the control and a significant reduction in the GFP accumulation after the additional  
204 sulfide treatment was observed resulting in protein levels lower than those detected in  
205 the control. Quantification of the ratio free GFP/GFP-ATG8 under each condition  
206 showed that ABA induced the autophagic flux and that this ABA-induced autophagy  
207 was repressed by NaHS (Figure 2B). These findings and the proteomic data suggest that  
208 sulfide is a negative regulator of bulk autophagy independently of the condition used to  
209 induce this catabolic process, including at least nutrient limitation (Alvarez et al., 2012;  
210 Laureano-Marin et al., 2016a) and ABA-dependent stress (this study). Furthermore,  
211 persulfidation appears to be the mechanism of action of sulfide and the AtATG4a  
212 protease may be one of the specific targets.

213

## 214 **Persulfidation of AtATG4a at Cys170**

215

216 To demonstrate the persulfidation-based modification of Cys residues in AtATG4a,  
217 recombinant protein was purified, subjected to the tag-switch procedure, and analyzed  
218 by immunoblotting using anti-biotin antibodies (Aroca et al., 2017a). A biotin-labeled  
219 protein band corresponding to AtATG4a was clearly detected by the antibody.  
220 Moreover, when AtATG4a was pretreated with DTT to reduce the persulfide residues,  
221 the biotin-labeled protein bands were not detected (Figure 3A). These results clearly  
222 indicate that AtATG4a undergoes persulfidation *in vitro*. To identify the Cys residue  
223 that can be modified by persulfidation, recombinant AtATG4a was analyzed by liquid  
224 chromatography (LC)-tandem mass spectrometry (MS/MS). The protein was digested  
225 with trypsin under nonreducing conditions in the absence of alkylating agents to avoid  
226 the reduction or modification of the persulfide residues. The digested peptides were  
227 analyzed to detect a 32 Da molecular mass increase in the fragmentation spectrum. The  
228 identified peptides included DTTYTSDVNWGCMIR that showed a persulfidation  
229 modification of Cys170 (Figure 3B). AtATG4a protein was identified with a sequence  
230 coverage of 97%, and no other persulfidated peptides were detected despite the presence  
231 of other eleven Cys residues in the primary structure (Figure 3C). Cys170 is located in  
232 the highly conserved catalytic site of ATG4 proteins from various organisms (Satoo et  
233 al., 2009; Perez-Perez et al., 2014; Perez-Perez et al., 2016) suggesting that the  
234 modification by persulfidation may have an important impact on the AtATG4a  
235 proteolytic activity and biological function.

236

## 237 ***In Vitro* Processing of CrATG8 by AtATG4a**

238

239 To determine whether modification of AtATG4 by persulfidation has an effect on its  
240 biological activity, an *in vitro* assay using CrATG8 from *C. reinhardtii* as a substrate  
241 was established (Perez-Perez et al., 2010). CrATG8 was previously used to monitor the  
242 activity of yeast ATG4 (Perez-Perez et al., 2010; Perez-Perez et al., 2014). ATG4  
243 processes ATG8 at a conserved glycine residue located at the C-terminus of the protein  
244 (Kirisako et al., 2000). Arabidopsis contains nine different ATG8 isoforms, none of  
245 which has more than five amino acid residues after the conserved glycine (Doelling et  
246 al., 2002). In contrast, CrATG8 harbors a 14-amino acid extension after the glycine, and  
247 CrATG8 processing can be easily monitored by Coomassie Blue-stained SDS-PAGE

248 due to differences in mobility between the unprocessed and processed CrATG8 forms  
249 (Supplemental Figure 1). When purified AtATG4a was incubated with CrATG8 in the  
250 presence of DTT, the processed protein with the same mobility as a truncated form  
251 lacking the last 14 amino acids (CrATG8<sup>G120</sup>, referred to as pCrATG8) was detected  
252 (Figure 4A). Therefore, AtATG4a was active and was able to process CrATG8 at its C-  
253 terminal Gly validating the ATG4 processing activity assay. The results indicated that  
254 AtATG4a activity was increased in a time-dependent manner and required a reducing  
255 agent to adopt the monomeric form required for the activity (Figure 4A), as described  
256 previously in other systems (Perez-Perez et al., 2010).

257 To analyze the effect of a reducing agent on AtATG4a activity, the *in vitro* assay  
258 in the presence or in the absence of different DTT or TCEP concentrations was  
259 performed. In the absence of DTT and TCEP, recombinant AtATG4a was in an  
260 oligomeric form that was retained in the upper part of the acrylamide gel. Increasing  
261 concentrations of the reducing agent enhanced the monomerization of recombinant  
262 AtATG4a and consequently the processing of CrATG8 by AtATG4a (Figure 4B and  
263 4C). Therefore, properties of Arabidopsis ATG4a were similar to those of the  
264 Chlamydomonas and yeast ATG4 (Perez-Perez et al., 2014; Perez-Perez et al., 2016).  
265 Interestingly, TCEP was more efficient than DTT in the activation of CrATG8  
266 cleavage, showing the maximum level of ATG4 activity at 0.5 mM TCEP while two  
267 orders of magnitude higher DTT concentration was required for optimal activity (Figure  
268 4B and 4C).

269

### 270 **Sulfide inhibits the proteolytic activity of AtATG4a**

271

272 A suitable ATG4 enzyme activity assay was developed and used to study whether  
273 persulfidation plays a role in the regulation of this activity. Thus, purified recombinant  
274 AtATG4a was pretreated with TCEP to produce an active enzyme and then incubated  
275 with increasing concentrations of NaHS as a sulfide donor. The ATG4 activity-  
276 dependent CrATG8 processing was determined using the Coomassie-stained gel  
277 method (Figure 5A). An increase in the accumulation of the unprocessed CrATG8 form  
278 was detected when AtATG4a was incubated in the presence of NaHS at a concentration  
279 as low as 0.1 mM. ATG4 activity was determined as the ratio of the band intensity of  
280 the processed CrATG8 to the sum of the intensities of the unprocessed and processed  
281 CrATG8; the data indicate that 0.1 mM NaHS significantly inhibits the ATG4 activity

282 to approximately 40% of the activity in the absence of sulfide (Figure 5B). Interestingly,  
283 analysis of the aggregation state of AtATG4a in the presence of the sulfide donor  
284 demonstrated that NaHS has different effects on monomerization and activity of  
285 AtATG4a (Figure 5C). Sulfide did not promote the oligomerization of the active  
286 monomeric AtATG4a to the same extent as it inhibited ATG4 proteolytic activity under  
287 the conditions used in the assays. Concentrations of NaHS from 0.1 to 0.5 mM did not  
288 significantly increase the abundance of high molecular weight and inactive oligomers of  
289 AtATG4a (Figure 5C). These results indicate that sulfide donor inhibits AtATG4a  
290 activity but does not directly influence the aggregation state of the protein in contrast to  
291 the effect of DTT or thioredoxin on yeast and *C. reinhardtii* ATG4 proteins (Perez-  
292 Perez et al., 2014; Perez-Perez et al., 2016).

293 Recent studies have questioned whether NaHS can be the sulfurating molecule  
294 instead of the proposed polysulfide and persulfide molecules. These molecules contain  
295 sulfane sulfur, the form of sulfur ( $S^0$ ) with the ability to reversibly attach to other sulfur  
296 atoms. Most of the reported biological activity associated with sulfide may be due to  
297 persulfides, which are considered responsible for intracellular signal transduction  
298 through persulfidation *in vivo* (Toohey, 2011; Ida et al., 2014; Mishanina et al., 2015).  
299 Thus, assays similar to those described above were performed using various  
300 concentrations of polysulfide  $Na_2S_4$  used as a sulfur donor. Our results indicated that  
301 polysulfide inactivates AtATG4a more efficiently than NaHS (Figure 6A and 6B).  
302 Concentrations of  $Na_2S_4$  three orders of magnitude (10-50  $\mu$ M) lower than those of  
303 NaHS were necessary to achieve a similar inhibition, and complete inactivation of the  
304 enzyme was observed at 100  $\mu$ M  $Na_2S_4$ . Furthermore, polysulfides were more active in  
305 promoting the aggregation of AtATG4a, and the differences in the effects on activity  
306 and oligomerization were not as pronounced as those observed with NaHS (Figure 6C).

307 Collectively, our results indicate that sulfide can inhibit the ATG4 proteolytic  
308 activity and that this inhibition is independent on the ATG4 aggregation state, at least at  
309 low concentrations of sulfurating species. Our results also suggest that this inhibitory  
310 effect is mediated by specific persulfidation of the catalytic Cys170 residue. Site-  
311 directed mutagenesis of this catalytic cysteine inactivates ATG4 activity in all tested  
312 systems and conditions (Scherz-Shouval et al., 2007; Shu et al., 2010; Perez-Perez et al.,  
313 2014; Perez-Perez et al., 2016), and therefore the mutant enzyme cannot be used to test  
314 the inhibitory effect of sulfide.

315 To examine the impact of posttranslational modification of Cys170 by persulfidation  
316 on the interaction between AtATG4a and its substrate AtATG8a, 3D homology  
317 modelling was performed using the structure of the *Homo sapiens* HsATG4b-LC3  
318 complex (Satoo et al., 2009). AtATG4a shares up to 33.4% sequence identity with  
319 HsAtg4B (E-value  $7.3 \times 10^{-90}$ ) and AtATG8a shares up to 59.4% sequence identity with  
320 HsLC3 (E-value  $1.8 \times 10^{-40}$ ) with conserved residues covering the whole sequence.  
321 Persulfidation of Cys170 in the AtATG4a-AtATG8a protein complex caused  
322 conformational changes and intramolecular rearrangements of the catalytic site (Figure  
323 7A) influencing substrate recognition. Addition of the –SH group to Cys170 induced an  
324 unfavorable steric effect particularly affecting the His366 residue since the imidazole  
325 C $\delta$ 2 and N $\epsilon$ 2 atoms are 2.9 Å and 3.4 Å from the S atom of Cys170, respectively. The  
326 additional sulfur and hydrogen atoms have a covalent radius of 1.02 Å and 0.37 Å,  
327 respectively (Figure 7B). Therefore, this cysteine modification can inhibit the activity of  
328 the plant AtATG4a protein.

329 Interestingly, the simulation of surface electrostatic potential reveals the differences  
330 between HsATG4b-LC3 and AtATG4a-AtATG8a protein complexes; specifically, the  
331 electrostatic potential surface around the catalytic site of the human complex is more  
332 electronegative compared to that of the Arabidopsis complex (Supplemental Figure 2).  
333 However, cysteine persulfidation does not perturb the charge, since the additional –SH  
334 group is a neutral contribution. A closer look at the catalytic cavity region suggests that  
335 it is somewhat smaller and less exposed to the solvent in Arabidopsis compared to the  
336 human homologue likely hampering the accessibility of the substrate. Overall, these  
337 data suggest that inhibition of the processing activity of Arabidopsis AtATG4a may be  
338 due to a conformational change of the catalytic site induced by persulfidation.

339

#### 340 **Endogenous Arabidopsis ATG4 processes CrATG8 for conjugation**

341

342 Our results indicate that sulfide can regulate ATG4 proteolytic activity through  
343 persulfidation of a specific cysteine residue. This conclusion is based on *in vitro*  
344 experiments. If sulfide has a biological role in the control of ATG4 activity in living  
345 plants, the inhibitory effect of sulfide should be reversible. To explore this hypothesis,  
346 active AtATG4a was inhibited by a high concentration of Na<sub>2</sub>S<sub>4</sub> to promote complete  
347 inactivation and to determine the extent of reversion by reduction of all persulfide  
348 residues with TCEP. The reactivation of AtATG4a was monitored as the ratio of the

349 protein band intensities of unprocessed and processed CrATG8 (Figure 6D). The results  
350 clearly confirm that the inhibition of ATG4 proteolytic activity by sulfide is reversible,  
351 suggesting that it may play a role in the control of ATG4 *in vivo*.

352 To determine whether sulfide regulation of ATG4 also occurs *in vivo*, ATG4 enzyme  
353 activity was detected in Arabidopsis leaves using the addition of exogenous CrATG8 to  
354 leaf protein extracts. Immunoblot analysis using antibodies against CrATG8 indicated  
355 that CrATG8 was efficiently processed by incubation with Arabidopsis leaf protein  
356 extracts (Figure 8A, right part). To confirm the specificity of the CrATG8 cleavage  
357 assay, Arabidopsis leaf protein extracts were incubated with a mutant of CrATG8 with  
358 conserved Gly-120 replaced by Ala (G120A). This CrATG8 mutant is not processed by  
359 ATG4 (Perez-Perez et al., 2010; Perez-Perez et al., 2016). When G120A was used as  
360 the substrate, the processed form was not detected, demonstrating the specificity of the  
361 endogenous ATG4 activity in Arabidopsis (Figure 8A, left part). Moreover, in addition  
362 to full-length and processed CrATG8, the antibodies specifically recognized other bands  
363 with faster mobility than pCrATG8 (Figure 8, asterisks). These bands were exclusively  
364 detected when wild type CrATG8, but not the G120A mutant, was used in the assay and  
365 they apparently correspond to the conjugated form of CrATG8 protein, as demonstrated  
366 previously in *Chlamydomonas* (Perez-Perez et al., 2010). Incubation of the Arabidopsis  
367 protein extract with the processed form of the CrATG8 (pCrATG8), which does not  
368 require cleavage by ATG4 and can be conjugated to PE (Supplemental Figure 3),  
369 confirmed that the faster mobility bands correspond to lipidated forms. The antibodies  
370 detected mainly an intense protein band that was progressively accumulated with  
371 incubation time and fully lipidated at the shortest time of incubation with the extracts  
372 under autophagy-activating conditions induced by nitrogen deficiency (Supplemental  
373 Figure 3). Therefore, our data demonstrated that the Arabidopsis protein extracts  
374 contain all the active proteins required for the conjugation of ATG8 and efficiently  
375 recognize CrATG8, thus validating the results of the ATG4 activity assay in the cell-  
376 free total extract.

377 To confirm the conclusion that Arabidopsis ATG4 proteins catalyze the processing  
378 of CrATG8 in the cell-free total extract assay, the ATG4 enzyme activity of the  
379 Arabidopsis protein extracts prepared from the *atg4ab* double-mutant seedlings was  
380 assayed (Supplemental Figure 4) (Yoshimoto et al., 2004; Chung et al., 2010). When  
381 CrATG8 was incubated with the Arabidopsis *atg4ab* protein extract, the processed form  
382 of CrATG8 was not detected even after extended incubation. Similarly, when protein

383 extracts were prepared from nitrogen-limited seedlings, the immunoblot analysis  
384 revealed a prominent protein band corresponding to the lipidated form of CrATG8 only  
385 in the presence of protein extracts from wild-type plants but not from the *atg4ab* mutant  
386 (Figure 8B).

387 Therefore, our data show that endogenous Arabidopsis ATG4 proteins recognize the  
388 cleavage site of the Chlamydomonas ATG8 substrate, which is efficiently processed in  
389 the cell-free enzymatic assay.

390

### 391 **Sulfide reversibly inhibits the ATG4 activity in Arabidopsis seedlings**

392

393 The effect of a sulfurating species on endogenous Arabidopsis ATG4 proteins was  
394 investigated to confirm the results obtained in *in vitro* analysis. Leaf protein extracts  
395 were treated with polysulfide, and CrATG8-processing activity was compared with that  
396 in the untreated extract. A pronounced decrease in the ATG4 activity was observed  
397 when the Arabidopsis extract was pretreated with Na<sub>2</sub>S<sub>4</sub> (Figure 9A). Additionally,  
398 treatment of the Arabidopsis leaf protein extract with the alkylating agent  
399 iodoacetamide inhibited ATG4 activity as expected because ATG4 is a Cys protease  
400 and its activity is dependent on the catalytic Cys; this effect was similar to the effect of  
401 polysulfide (Figure 9A, left panel). Thus, these findings strongly suggest that sulfide  
402 negatively regulates ATG4 activity *in vivo*, at least the cleavage activity of the C-  
403 terminal extension of ATG8. Reversibility of the inhibitory effect of polysulfide was  
404 also analyzed. When the polysulfide-incubated Arabidopsis extract was treated with  
405 TCEP as a reducing agent to reduce the persulfide-modified cysteine residues in the  
406 protein extract, a significant difference in the activity was detected compared with that  
407 in the polysulfide-treated extract (Figure 9A, right panel). When the extract was  
408 incubated with Na<sub>2</sub>S<sub>4</sub>, the processed CrATG8 form was barely detected; however,  
409 incubation with TCEP significantly increased the abundance of this band, suggesting  
410 that sulfide may inhibit Arabidopsis ATG4 activity in a reversible manner.

411 To characterize the inhibition of ATG4 proteolytic activity by sulfide, the effect of  
412 polysulfide on the ATG4 activity was assayed under basal and autophagy-inducing  
413 conditions. Two different established conditions of autophagy induction were tested:  
414 nitrogen deficiency, which has been extensively characterized previously (Doelling et  
415 al., 2002; Hanaoka et al., 2002; Xiong et al., 2005; Phillips et al., 2008; Guiboileau et  
416 al., 2013; Laureano-Marin et al., 2016aa), and osmotic stress (Liu et al., 2009) imposed

417 by the addition of mannitol to the growth medium, which induces ABA-dependent  
418 signaling pathway. The processed form of CrATG8 was detected in total extracts under  
419 the control and autophagy-activating conditions, and sulfide inhibited endogenous  
420 ATG4 activity under both conditions (Figure 9B). The faster-mobility protein band  
421 corresponding to the lipidated form of CrATG8 was more prominent under nitrogen  
422 limitation than osmotic stress; however, sulfide treatment decreased the accumulation of  
423 the conjugated forms of CrATG8 under both conditions.

424

425

## 426 **DISCUSSION**

427

428 Accumulating evidence emphasizes the importance of autophagy in plant growth and  
429 development. This catabolic process is highly dynamic and occurs at the basal levels to  
430 maintain cellular homeostasis during growth; however, autophagy is fine-tuned to  
431 adjust plant metabolism to internal and external perturbations. Various regulators of  
432 autophagy have been identified in plant systems, such as the energy sensor Snf1-related  
433 protein kinase 1 (SnRK1), the kinase Target of Rapamycin (TOR), the TOR  
434 downstream substrate ATG1 kinase complex, and the ER stress sensor inositol-  
435 requiring enzyme-1 (IRE1) (Marshall and Vierstra, 2018b; Soto-Burgos et al., 2018).

436 Other regulators of autophagy, such as hydrogen sulfide, have been identified  
437 although the details of the molecular mechanism of action of these regulators remain  
438 poorly understood. In the animal systems, interactions of sulfide with autophagy have  
439 been described in various pathologies; depending on the disease, sulfide can either  
440 suppress or activate autophagy. In all cases, hydrogen sulfide has protective effects  
441 (Sen, 2017; Wang et al., 2017; Wu et al., 2018). Despite substantial progress, the exact  
442 mechanism of autophagy regulation by sulfide in mammals remains unknown. In plants,  
443 particularly in *Arabidopsis*, the interplay between sulfide and autophagy has been  
444 shown, and progress in understanding of the mechanism has been obtained. Hydrogen  
445 sulfide generated in the cytosol functions as a signaling molecule negatively regulating  
446 autophagy independently of the nutritional conditions. Furthermore, sulfide was shown  
447 to repress autophagy via a mechanism that is independent of redox conditions (Alvarez  
448 et al., 2012; Laureano-Marin et al., 2016a).

449 Sulfur and autophagy are also linked by the mechanism of *Arabidopsis* sensing of the  
450 sulfur-containing amino acid cysteine. Two different pathways have been identified for

451 sensing of its carbon/nitrogen precursor and its sulfur precursor. The sulfur precursor is  
452 transduced to TOR by downregulation of glucose metabolism; therefore, sulfide  
453 increases glucose levels and TOR kinase activity, downregulating autophagy (Dong et  
454 al., 2017). This study demonstrated that cytosolic sulfide is not the signal responsible  
455 for the regulation but does not exclude chloroplast sulfide as the signaling molecule. In  
456 fact, a proteomic study showed that other sulfurating species in addition to the cytosolic  
457 sulfide can be responsible for regulation of diverse biological processes (Aroca et al.,  
458 2017a).

459 The data of the present study emphasize sulfide regulation of autophagy. Our  
460 findings indicate that ABA activates autophagy and hydrogen sulfide downregulates  
461 this catabolic process. A link between autophagy and ABA was previously described  
462 through the Arabidopsis multistress regulator TSPO, a tryptophan-rich sensory protein-  
463 related. ABA induces TSPO as a heme scavenger, which binds the excessive or  
464 deleterious heme and then is targeted for degradation through autophagy (Vanhee and  
465 Batoko, 2011; Vanhee et al., 2011). Other connections between autophagy and ABA  
466 signaling via TOR have been described. Under nonstressed conditions, TOR  
467 phosphorylation of ABA receptors leads to inactivation of SnRK2 kinases and disrupts  
468 ABA signaling. Under abiotic stress conditions, ABA activates SnRK2 that  
469 phosphorylates RAPTOR resulting in the inhibition of TOR and consequential  
470 activation of autophagy (Wang et al., 2018).

471 Previous studies have shown that the main mechanism of action of sulfide involves  
472 persulfidation of reactive cysteine residues of the target proteins resulting in changes in  
473 enzyme structure, activity and subcellular localization previously demonstrated in  
474 several target plant proteins (Aroca et al., 2015; Aroca et al., 2017b; Aroca et al., 2018).  
475 A proteomic analysis performed on mature leaves from Arabidopsis plants grown under  
476 nonstress conditions revealed that a high proportion of the whole Arabidopsis proteome  
477 may undergo persulfidation under the basal conditions (Aroca et al., 2017a). In this  
478 study, a comparative and quantitative proteomic analysis has been performed on ABA-  
479 treated leaves to determine whether persulfidation mechanism is involved in sulfide  
480 regulation of the ABA signaling pathways. Significant differences in the levels of  
481 persulfidation were observed after ABA treatment compared to that under the control  
482 conditions. Surprisingly, the protein with the lowest level of persulfidation after 3 h  
483 ABA treatment was identified as Cys-type protease AtATG4a (5.20-fold change,  
484  $p < 0.05$ , control *versus* 3h ABA), and even after 6 h of ABA treatment, the reduction in

485 the level of persulfidation remained very significant (2.46-fold change,  $p < 0.05$ , control  
486 *versus* 6 h ABA). These data suggest that AtATG4a may be a target of persulfidation  
487 and that this posttranslational modification may be the molecular mechanism mediating  
488 sulfide regulation of autophagy. A detailed analysis of the ABA-triggered changes in  
489 the persulfidation proteome will be performed in a future study. Our results  
490 demonstrated that ATG4 proteolytic activity in Arabidopsis is reversibly regulated by  
491 sulfide, and this regulation effectively controls the progression of autophagy. Thus, our  
492 findings contribute to the understanding of the mechanism of regulation of autophagy  
493 by sulfide in the plant systems and add another level of regulation to this process.

494 The AtATG4a protease contains a specific site of persulfidation detected by the tag-  
495 switch procedure and confirmed by mass spectrometry. The specifically persulfidated  
496 cysteine residue is Cys170, which is a part of the characteristic catalytic triad Cys-His-  
497 Asp of cysteine proteases (Sugawara et al., 2005). Comparison of the amino acid  
498 sequences of ATG4s from various biological systems indicated low similarity although  
499 the amino acids required for the cysteine protease activity, including the catalytic  
500 Cys170, are highly conserved. Interestingly, Cys170 is the only Cys residue that is  
501 conserved in all known ATG4s (Supplemental Figure 5) (Perez-Perez et al., 2014;  
502 Perez-Perez et al., 2016; Seo et al., 2016). In contrast, redox regulation of specific Cys  
503 residues has been detected in ATG4 from human, yeast, and *Chlamydomonas*.  
504 However, these residues are not conserved in various organisms and therefore the  
505 details of the regulatory mechanisms may be different. In humans, HsATG4a and  
506 HsATG4b proteases are the targets of reversible oxidation by  $H_2O_2$ , and the cysteine  
507 residue Cys81 located close to the catalytic Cys residue (Cys77, analogous to Cys170 in  
508 Arabidopsis) was shown to be critical for this regulation (Scherz-Shouval et al., 2007).  
509 Recently, Cys292 and Cys361 have been shown to be HsATG4b sites essential for  
510 reversible oxidative modification (Zheng et al., 2020). Redox regulation of the yeast  
511 ScATG4 protein is due to the formation of a disulfide bond between the noncatalytic  
512 residues Cys338 and Cys394, which is thioredoxin-dependent (Perez-Perez et al., 2014).  
513 In *Chlamydomonas reinhardtii*, CrATG4 activity depends on the formation of a single  
514 disulfide bond regulated by the NADPH/thioredoxin system; however, only Cys400,  
515 which is the equivalent to Cys338 in yeast, has been demonstrated to be required for  
516 redox regulation of the algal CrATG4 enzyme (Perez-Perez et al., 2016). In  
517 Arabidopsis, the activity of AtATG4a and AtATG4b is reversibly inhibited *in vitro* by  
518 reactive oxygen species (Woo et al., 2014), although redox regulation of the critical

519 cysteine residues was not reported. Additionally, other posttranslational modifications  
520 of cysteine residues of ATG4 proteases have been described, such as S-nitrosylation of  
521 HsATG4b at Cys189 and Cys292, though these two residues are not conserved in the  
522 HsATG4a amino acid sequence (Li et al., 2017). Therefore, persulfidation of the  
523 catalytic Cys residue of cysteine proteases ATG4 can be a posttranslational  
524 modification conserved in various biological systems.

525 Because the target residue of persulfidation involves the active site, an effect of the  
526 sulfide donor molecules on the enzymatic activity of AtATG4a was anticipated. In fact,  
527 a 3D modelling analysis predicted that the addition of a sulfur atom to the -SH group of  
528 Cys170 can cause unfavorable effects on the catalytic site of AtATG4a that should  
529 affect substrate recognition and impair the enzyme activity. To test this hypothesis, a  
530 heterologous activity assay was developed using CrATG8 as a substrate similar to  
531 previously reported assays (Perez-Perez et al., 2014; Seo et al., 2016). Our results  
532 indicate that the plant protease is functional and can process the algal substrate.

533 Our findings demonstrate that sulfide plays a specific role in the regulation of ATG4  
534 enzymatic activity. The sulfide donor molecules used in this study, such as hydrosulfide  
535 and tetrasulfide, significantly inactivate AtATG4a cleavage activity even at relatively  
536 low concentrations, being polysulfide the most efficient inhibitor. The chemical  
537 mechanism of the reaction of the thiol groups with the sulfide molecule remains a  
538 matter of debate. H<sub>2</sub>S cannot directly react directly with thiols, and the cysteine group  
539 must be partially oxidized (converted to disulfide, glutathiolated, S-nitrosylated, or to  
540 sulfenic acid) prior to sulfide attack. Alternatively, certain chemical studies have  
541 demonstrated that sulfane sulfur (S<sup>0</sup>) of the polysulfide molecule is responsible for the  
542 production of persulfide during interaction with the thiol group (Toohey, 2011; Kimura,  
543 2015; Mishanina et al., 2015). This phenomenon can explain why polysulfide is a more  
544 potent inhibitor of ATG4 activity than hydrosulfide. Moreover, the inhibitory effect of  
545 low concentrations of sulfide on AtATG4a activity compatible with the *in vivo*  
546 conditions is reversible by a reducing agent suggesting a biological role of this effect.  
547 Interestingly, an enzymatic mechanism of reversing persulfidation by the thioredoxin  
548 system has been demonstrated in animal systems (Wedmann et al., 2016; Doka et al.,  
549 2020). Thus, it is plausible that the thioredoxin system also functions in plants to  
550 modulate the activity of AtATG4.

551 The biological significance of sulfide regulation of autophagy through reversible  
552 inhibition of ATG4 protease is reinforced by the assays in Arabidopsis leaves under

553 basal and autophagy-inducing conditions. Our experimental system was shown to be  
554 suitable for specific assay of Arabidopsis ATG4 processing activity by using various  
555 experimental approaches. Endogenous plant ATG4 cysteine proteases specifically  
556 recognize the Gly120 cleavage site in the substrate from green algae based on the  
557 experiment with the G120A mutant of the CrATG8 substrate. The processed form was  
558 not detected when the Arabidopsis protein extracts were deficient in ATG4a and  
559 ATG4b enzymes, demonstrating the specificity of our experimental system. The  
560 endogenous Arabidopsis ATG4 proteins mimic the effect of sulfurating molecules on  
561 AtATG4a *in vitro*, including significant inhibition by the sulfide donor and reversal by a  
562 reducing agent. A significant increase in the overall ATG4 protease activity in  
563 Arabidopsis was detected under autophagy-inducing conditions, including nitrogen  
564 starvation and osmotic stress. Thus, a correlation was detected between the progress of  
565 autophagy and the ATG4 enzymatic activity estimated using the heterologous assay  
566 method. Additionally, the inhibitory effect of sulfide on the protease activity was  
567 observed under the conditions of induced autophagy. Overall, our findings suggest that  
568 negative regulation of the progress of autophagy by sulfide is mediated by specific  
569 persulfidation of cysteine protease ATG4. However, additional targets of sulfide cannot  
570 be ruled out and further analysis is needed.

571 In conclusion, our data suggest a new level of regulation of ATG4 activity by sulfide.  
572 Based on our findings, we propose that intracellular sulfide maintains high levels of  
573 persulfidation of the ATG4 pool under basal conditions, resulting in the inhibition of  
574 ATG4 proteolytic activity. ATG4 inhibition limits the formation of ATG8-PE adducts  
575 and consequently *de novo* synthesis of autophagosomes. An increase in the intracellular  
576 level of ABA transiently reduces the level of persulfidation of the ATG4 population and  
577 then activates the protease activity of the enzyme to process ATG8 that can be further  
578 lipidated (Figure 10).

579  
580  
581  
582

## 581 **METHODS**

### 583 **Plant Material, Treatments and Protein Extraction**

584 Plant growth conditions were 16 h of light ( $120 \mu\text{E m}^{-2} \text{s}^{-1}$ ) at 22°C and 8 h of dark at  
585 20°C. The *Arabidopsis thaliana* wild-type and the *atg4ab* mutant (Nottingham  
586 Arabidopsis Stock Center) seeds were sown on Murashige and Skoog (MS) solid  
587 medium containing 0.8% (w/v) agar, synchronized at 4°C for 2 d, and incubated

588 vertically in a growth chamber (LUMILUX Cool White bulbs). For exposure to the  
589 nitrogen-starvation conditions, nitrogen-deficient MS medium was prepared by  
590 replacing nitrate salts with chloride salts. For mannitol treatment, 300 mM was added to  
591 the MS medium. One-week-old seedlings were transferred to nitrogen-deficient or  
592 mannitol-containing MS solid medium for an additional 4 d of growth.

593 For proteomic analysis, wild-type *Arabidopsis* plants were grown in soil for 30 days,  
594 and then sprayed with water (control conditions), or 50  $\mu$ M ABA for 3 and 6 h. To  
595 assess the autophagic activity, one-week-old *Arabidopsis* seedlings overexpressing  
596 GFP-ATG8e (Xiong et al., 2007) were transferred to the MS liquid medium and treated  
597 with 50  $\mu$ M ABA for 3 and 6 h and with 200  $\mu$ M NaHS for 1 h.

598 *Arabidopsis* material (200 mg) was ground in liquid nitrogen with 400 mL of  
599 extraction buffer (100 mM Tris-HCl, pH 7.5, 400 mM sucrose, 1 mM EDTA, 0.1 mM  
600 phenylmethylsulfonyl fluoride (PMSF)) using a mortar and pestle. After centrifugation  
601 at 500 g for 10 min at 4°C, the supernatant was used as the *Arabidopsis* protein extract.

602

#### 603 **Persulfidated Protein Quantitation by Label-free SWATH-MS Acquisition and** 604 **Analysis**

605 Protein samples from three biological replicates (independent pools) of leaf tissues  
606 treated with ABA for 0 h (control sample), 3 h and 6 h were isolated and 1 mg of  
607 protein per sample was used for the tag-switch labeling for enrichment of persulfidated  
608 proteins as described (Aroca et al, 2017). After elution from the streptavidin beads, the  
609 proteins were precipitated by TCA/acetone. Precipitated samples were resuspended in  
610 50 mM ammonium bicarbonate with 0.2% Rapigest (Waters) for protein determination.  
611 Protein (50  $\mu$ g) was digested with trypsin as described previously (García et al., 2019;  
612 Vowinckel et al., 2014), and the SWATH-MS analysis was performed at the Proteomic  
613 Facility of the Institute of Plant Biochemistry and Photosynthesis, Seville, Spain. A  
614 data-dependent acquisition (DDA) approach using nano-LC-MS/MS was initially  
615 performed to generate the SWATH-MS spectral library as described by García et al.,  
616 (2019).

617 The peptide and protein identifications were performed using Protein Pilot software  
618 (version 5.0.1, Sciex) with the Paragon algorithm. The search was conducted against a  
619 Uniprot proteome (June 2017, release), and the corresponding reversed entries and  
620 common contaminants were assembled in the FASTA format using ProteinPilot

621 software v5.0.1 (AB Sciex) with the Paragon algorithm. Samples were input as  
622 unlabeled with no special factors, trypsin digested and MSBT alkylated. The  
623 automatically generated report in ProteinPilot was manually inspected for FDR (false  
624 discovery rate) cut-off proteins and only proteins identified at  $FDR \leq 1\%$  were  
625 considered for output and subsequent analysis.

626 For relative quantification using SWATH analysis, the same samples used to  
627 generate the spectral library were analyzed using a data-independent acquisition (DIA)  
628 method. Each sample (2  $\mu$ L) was analyzed using SWATH-MS acquisition method on  
629 the LC-MS equipment with the LC gradient as described. The method consisted of  
630 repeated acquisition cycles of TOF MS/MS scans (230 to 1500 m/z, 60 ms acquisition  
631 time) of 60 overlapping sequential precursor isolation windows of variable width (1 m/z  
632 overlap) covering the 400-1250 m/z mass range from a previous TOF MS scan (400-  
633 1250 m/z, 50 ms acquisition time) for each cycle. The total cycle time was 3.7 s.

634 Autocalibration of the equipment and chromatographic conditions were controlled by  
635 an injection of a standard of digested  $\beta$ -galactosidase from *E coli* between the replicates.

636 SWATH MS spectra alignment was performed with the PeakView 2.2 (Sciex)  
637 software with the MicroApp SWATH 2.0 using the reference spectral library generated  
638 as described above. Two DIA raw files for each biological replicate were loaded in  
639 unison using the following parameters: 10 peptides, 7 transitions, peptide confidence  
640  $>99\%$ , 1% FDR including shared peptides, and XIC width set at 0.05 Da. After data  
641 processing, three distinct files were exported for subsequent quantification. The  
642 processed mrkvw files containing protein information from PeakView were loaded into  
643 MarkerView (Version 1.2.1, AB Sciex) for normalization of protein intensity (peak  
644 area) for all runs using the built-in total ion intensity sum plug-in.  $\text{Log}_2$  transformation  
645 was performed prior to statistical analysis. A histogram plot was used to check the  
646 normality of distribution of each technical replicate. Mean values of protein expression  
647 were used for calculation of fold change (FC). Proteins with adjusted  $p < 0.05$  and  
648  $FC \geq 1.5$  were considered differentially expressed.

649 The mass spectrometry proteomic data have been deposited to the ProteomeXchange  
650 Consortium via the PRIDE (Vizcaino et al, 2016) partner repository with the identifier  
651 PXD019802.

652

653 **Expression of AtATG4a in *Escherichia coli***

654 Total RNA was extracted from wild-type Arabidopsis leaves using an RNeasy plant  
655 mini kit (Qiagen) and reverse-transcribed using an oligo (dT) primer and a SuperScript  
656 first-strand synthesis system for RT-PCR (Invitrogen). Subsequently, a 1,404 bp  
657 sequence encoding the full-length AtATG4a (At2g44140) protein was amplified by  
658 PCR using the primers ATG4-F: CACCATGAAGGCTTTATGTGA and ATG4-R:  
659 ATGACTGGCAAATGCTCTGA and the proofreading Platinum Pfx DNA polymerase  
660 (Invitrogen). The PCR conditions were as follows: a denaturation cycle of 2 min at 94°C  
661 followed by 30 amplification cycles of 15 s at 94°C, 30 s at 57°C, and 1 min at 68°C.  
662 The amplified cDNA was then ligated into the pENTR/D-TOPO vector using the  
663 pENTR directional TOPO cloning kit (Invitrogen) according to the manufacturer's  
664 instructions. Positive clones were identified by PCR and selected for plasmid DNA  
665 isolation. The *AtATG4a* cDNA was then cloned into the expression vector pDEST17  
666 using an *E. coli* expression system with gateway technology (Invitrogen), which  
667 generates a fusion protein with an N-terminal 6x His tag that was confirmed by  
668 sequencing; the expression was induced with L-arabinose in BL21-AI *E. coli* cells.

669

#### 670 **Purification of the Recombinant AtATG4a Protein**

671 The 6x His-tagged recombinant protein was isolated from 200 mL of BL21-AI *E. coli*  
672 cells that were cultured at 37°C to an optical density of 0.5 at 600 nm and induced with  
673 0.2% (w/v) L-arabinose for 2.5 h at 37°C. Prior to purification, His-tagged AtATG4a  
674 was solubilized with 6 M urea because the recombinant protein was contained in the  
675 inclusion bodies. Then, the protein was purified from the soluble fraction by nickel  
676 affinity chromatography using an Invitrogen Ni-NTA Purification System  
677 (ThermoFisher Scientific), according to the manufacturer's instructions. The purified  
678 protein was concentrated and desalted using 10 kD cutoff pore size centrifugal filter  
679 units (Millipore). The purity of the protein was confirmed by SDS-PAGE using 12%  
680 (w/v) polyacrylamide gels stained by Coomassie Blue.

681

#### 682 **Detection of Persulfidation on the Recombinant AtATG4a**

683 An untreated aliquot of the purified recombinant AtATG4a and another aliquot  
684 pretreated with 50 mM DTT for 30 min at 4°C to reduce all persulfide groups were  
685 precipitated with acetone for 20 min at -20°C and centrifuged at a maximum speed for  
686 20 min at 4°C. After acetone removal, the proteins were resuspended in 50 mM Tris-  
687 HCl (pH 8) buffer supplemented with 2.5% (w/v) SDS and subjected to the tag-switch

688 procedure as described previously (Aroca et al., 2017a). The CN-biotinylated proteins  
689 were then detected using an immunoblot assay as follows. The CN-biotinylated proteins  
690 were separated using nonreducing SDS-PAGE through 12% (w/v) polyacrylamide gels  
691 and transferred to polyvinylidene difluoride membranes (Bio-Rad) according to the  
692 manufacturer's instructions. The anti-biotin (Abcam, catalog # ab191354) and  
693 secondary antibodies (Bio-Rad, catalog # 170-6515) were diluted 1:500,000 and  
694 1:100,000, respectively, and ECL Select western blotting detection reaction (GE  
695 Healthcare) was used to detect the proteins using horseradish peroxidase-conjugated  
696 anti-rabbit secondary antibodies. For protein loading control, the membranes before  
697 immunodetection were stained with SYPRO Ruby (Invitrogen) to detect all protein  
698 bands.

699

#### 700 **Identification of Persulfidated Cys Residues of Recombinant AtATG4a Using** 701 **Mass Spectrometry**

702 Recombinant AtATG4a was separated using nonreducing SDS-PAGE through 12%  
703 (w/v) polyacrylamide gels, and the band corresponding to AtATG4a was manually  
704 excised from Coomassie-stained gels. Gel plugs were washed twice using 50 mM  
705 ammonium bicarbonate and acetonitrile and dried under a stream of nitrogen. Then,  
706 proteomics-grade trypsin (Sigma-Aldrich) at a final concentration of 16 ng/ $\mu$ l in 25%  
707 (v/v) acetonitrile/50 mM ammonium bicarbonate solution was added; the samples were  
708 digested at 37°C for 5 h. The reaction was stopped by adding 50% (v/v)  
709 acetonitrile/0.5% (v/v) trifluoroacetic acid for peptide extraction. The eluted tryptic  
710 peptides were dried by speed-vacuum centrifugation and resuspended in 6  $\mu$ l of 0.1%  
711 (v/v) formic acid in water. Digested peptides were subjected to nanoliquid  
712 chromatography electrospray ionization tandem mass spectrometry analysis using a  
713 nanoliquid chromatography system (ExcionLC AD, Sciex) coupled to a TripleTOF  
714 5600+ mass spectrometer (Sciex) with a spray ionization source. Mass spectrometry and  
715 MS/MS data of individual samples were processed using the Analyst TF 1.5.1 software  
716 (Sciex). Peptide mass tolerance was set to 25  $\mu$ D D<sup>-1</sup> and 0.05 D for fragment masses,  
717 and only one or two missed cleavages were allowed. Peptides with an individual M<sub>r</sub>  
718 search score  $\geq 20$  were considered correctly identified.

719

#### 720 ***In vitro* ATG4 Enzyme Activity Assay**

721 The typical reaction mixture contained 5  $\mu\text{M}$  recombinant AtATG4a, 5  $\mu\text{M}$  CrATG8  
722 (Perez-Perez et al., 2010), and 1 mM EDTA in Tris-buffered saline (50 mM Trizma  
723 base, 138 mM NaCl, and 27 mM KCl at pH 8). When indicated, AtATG4a was  
724 incubated in the presence of DTT, TCEP, NaHS,  $\text{Na}_2\text{S}_4$ , or iodoacetamide alone or in  
725 combination at the indicated times and concentrations. The reaction mixtures were  
726 incubated at 25°C, and the reaction was stopped by the addition of  $\beta$ -mercaptoethanol-  
727 free Laemmli sample buffer followed by 5 min boiling. The proteins were resolved  
728 using nonreducing SDS-PAGE through 15% (w/v) polyacrylamide gels and stained  
729 with Coomassie Brilliant Blue (Sigma-Aldrich). The gels were scanned with a GS-800  
730 densitometer (Bio-Rad), and the signals corresponding to the unprocessed and  
731 processed CrATG8 forms were quantified with the Quantity One software (Bio-Rad).  
732 The ATG4 activity (in arbitrary units) was calculated as the ratio of the band intensity  
733 of the processed CrATG8 to the sum of the intensities of the unprocessed and processed  
734 CrATG8. An activity value of 1 corresponds to the maximum value.

735

#### 736 **Assay of Endogenous ATG4 Enzyme Activity in Cell-Free Total Extract**

737 The *in vivo* assay of ATG4 activity in cell-free total extract was performed in a typical  
738 reaction mixture containing 40  $\mu\text{g}$  of leaf or 20  $\mu\text{g}$  of root protein extract and 0.05  $\mu\text{M}$   
739 purified unprocessed CrATG8, processed pCrATG8, or Gly-to-Ala mutant protein  
740 (G120A). When required, a sulfur donor ( $\text{Na}_2\text{S}_4$ ), a reducing agent (TCEP), or an  
741 alkylating agent (IAM) was added at the indicated concentrations. The reaction mixture  
742 was incubated at 25°C for the indicated time, stopped by addition of  $\beta$ -mercaptoethanol-  
743 free Laemmli sample buffer, and boiled for 5 min. Then, proteins were separated using  
744 nonreducing SDS-PAGE through 15% (w/v) polyacrylamide gels and transferred to  
745 nitrocellulose membranes (Bio-Rad) as described previously (Perez-Perez et al., 2010).  
746 Anti-CrATG8 (Pérez-Pérez et al., 2010) and secondary antibodies were diluted 1:3,000  
747 and 1:10,000, respectively. An ECL Select western blotting detection reaction (GE  
748 Healthcare) was used to detect the proteins. For protein loading control, the membranes  
749 before immunodetection were stained with Ponceau S (Sigma-Aldrich) to detect all  
750 protein bands.

751

#### 752 **Protein modeling**

753 3D homology modeling was driven by Modeller (Sali and Blundell, 1993) using the  
754 structure of the *Homo sapiens* Atg4B-LC3 complex (PDB ID: 2Z0E) (Sato et al., 2009)  
755 as a template. Molecular crystal X-ray structures and structural model of *Arabidopsis*  
756 *thaliana* AtATG4a-AtATG8a complex were inspected, analyzed and plotted with  
757 PyMol 1.4.1 (Schrodinger LLC). Surface electrostatic potentials were calculated and  
758 visualized using the PyMol 1.4.1 software.

759

#### 760 **Accession Numbers**

761 The mass spectrometry proteomic data have been deposited to the ProteomeXchange  
762 Consortium via the PRIDE partner repository with the identifier PXD019802. Sequence  
763 data from this article can be found in the EMBL/GenBank data libraries under the  
764 following accession numbers: *AtATG4a* (At2g44140), *AtATG4b* (At3g59950), *AtATG8a*  
765 (At4g21980) and *CrATG8* (Cre16.g689650.t1.1).

766

767

#### 768 **SUPPLEMENTAL DATA**

769 **Supplemental Figure 1.** C-Termini of the Chlamydomonas ATG8 proteins and nine  
770 Arabidopsis ATG8 proteins.

771 **Supplemental Figure 2.** Simulation of surface electrostatic potential distribution in the  
772 HsATG4b-LC3 protein complex (PDB ID: 2Z0E) and AtATG4a-AtATG8a 3D  
773 structural model.

774 **Supplemental Figure 3.** Conjugation of Chlamydomonas ATG8 processed by ATG4s  
775 proteases from Arabidopsis.

776 **Supplemental Figure 4.** Phenotypes of wild-type and *atg4ab* double-mutant seedlings  
777 under the basal and induced autophagy conditions.

778 **Supplemental Figure 5.** Alignment of amino acid sequences of ATG4 from various  
779 sources.

780 **Supplemental Figure 6.** Lower exposure of the GFP-blot shown in Figure 2.

781

782 **Supplemental Table 1.** Classification of the proteins with persulfidation level reduced  
783 after 3 h ABA treatment.

784 **Supplemental Table 2.** Protein list of the elements included in the bin of "proteins"  
785 with persulfidation level reduced after 3 h ABA treatment.

786

787 **Supplemental Dataset 1.** Spectral library

788 **Supplemental Dataset 2.** Proteins quantified using SWATH acquisition method in the  
789 control sample versus 3 h ABA treatment sample.

790 **Supplemental Dataset 3.** Proteins with different abundance in the control sample  
791 compared to that in the 3 h ABA treatment sample at p value <0.05.

792 **Supplemental Dataset 4.** Proteins quantified using SWATH acquisition method in the  
793 control sample versus 6 h ABA treatment sample.

794 **Supplemental Dataset 5.** Proteins with different abundance in the control sample  
795 compared to that in the 6 h ABA treatment sample at p value <0.05.

796

797

798

799

## 800 **ACKNOWLEDGMENTS**

801

802 This work was supported in part by the European Regional Development Fund through  
803 the Ministerio de Economía y Competitividad and the Agencia Estatal de Investigación  
804 grants BFU2015-68216-P and PGC2018-099048-B-I00 (to J.L.C.); grants BIO2015-  
805 74432-JIN and PID2019-110080GB-I00 (to M.E.P-P.); grants BIO2016-76633-P and  
806 PID2019-109785GB-I00, and Junta de Andalucía grant P18-RT-3154 (to C.G.), the  
807 Marie Skłodowska-Curie grant agreement No. 834120 (to A.A.), and Government of  
808 Aragón-FEDER grant E35\_17R (to I. Y.). A.M. L-M. and A. J-F. were supported by the  
809 Ministerio de Economía y Competitividad through the program of “Formación de  
810 Personal Investigador”. We want to thank Dr. Rocío Rodríguez for the Proteomics  
811 Services.

812

## 813 **AUTHOR CONTRIBUTIONS**

814

815 Á.A., A.M.L-M., M.E.P-P., I.Y., A. J-F. and I.M. performed research and analyzed the  
816 data. J.L.C. and L.C.R. designed research and analyze data. C.G. designed the research,  
817 analyzed the data, and wrote the article. All authors contributed to the discussion.

818

819

820 **REFERENCES**

821

- 822 **Alvarez C, Garcia I, Moreno I, Perez-Perez ME, Crespo JL, Romero LC, Gotor C** (2012)  
823 Cysteine-generated sulfide in the cytosol negatively regulates autophagy and  
824 modulates the transcriptional profile in Arabidopsis. *Plant Cell* **24**: 4621-4634.
- 825 **Aroca A, Gotor C, Romero LC** (2018) Hydrogen Sulfide Signaling in Plants: Emerging  
826 Roles of Protein Persulfidation. *Front Plant Sci* **9**.
- 827 **Aroca A, Benito JM, Gotor C, Romero LC** (2017a) Persulfidation proteome reveals the  
828 regulation of protein function by hydrogen sulfide in diverse biological  
829 processes in Arabidopsis. *J Exp Bot* **68**: 4915-4927.
- 830 **Aroca A, Schneider M, Scheibe R, Gotor C, Romero LC** (2017b) Hydrogen Sulfide  
831 Regulates the Cytosolic/Nuclear Partitioning of Glyceraldehyde-3-Phosphate  
832 Dehydrogenase by Enhancing its Nuclear Localization. *Plant Cell Physiol* **58**:  
833 983-992.
- 834 **Aroca Á, Serna A, Gotor C, Romero LC** (2015) S-Sulfhydration: A Cysteine  
835 Posttranslational Modification in Plant Systems. *Plant Physiol* **168**: 334-342.
- 836 **Calderwood A, Kopriva S** (2014) Hydrogen sulfide in plants: From dissipation of excess  
837 sulfur to signaling molecule. *Nitric Oxide* **41C**: 72-78.
- 838 **Chen S, Jia H, Wang X, Shi C, Wang X, Ma P, Wang J, Ren M, Li J** (2020) Hydrogen  
839 Sulfide Positively Regulates Abscisic Acid Signaling through Persulfidation of  
840 SnRK2.6 in Guard Cells. *Mol Plant*.
- 841 **Chung T, Phillips AR, Vierstra RD** (2010) ATG8 lipidation and ATG8-mediated  
842 autophagy in Arabidopsis require ATG12 expressed from the differentially  
843 controlled ATG12A AND ATG12B loci. *Plant J* **62**: 483-493.
- 844 **Doelling JH, Walker JM, Friedman EM, Thompson AR, Vierstra RD** (2002) The  
845 APG8/12-activating enzyme APG7 is required for proper nutrient recycling and  
846 senescence in Arabidopsis thaliana. *J Biol Chem* **277**: 33105-33114.
- 847 **Doka E, Ida T, Dagnell M, Abiko Y, Luong NC, Balog N, Takata T, Espinosa B,**  
848 **Nishimura A, Cheng Q, Funato Y, Miki H, Fukuto JM, Prigge JR, Schmidt EE,**  
849 **Arner ESJ, Kumagai Y, Akaike T, Nagy P** (2020) Control of protein function  
850 through oxidation and reduction of persulfidated states. *Sci Adv* **6**: eaax8358.
- 851 **Dong Y, Silbermann M, Speiser A, Forieri I, Linster E, Poschet G, Allboje Samami A,**  
852 **Wanatabe M, Sticht C, Teleman AA, Deragon JM, Saito K, Hell R, Wirtz M**  
853 (2017) Sulfur availability regulates plant growth via glucose-TOR signaling. *Nat*  
854 *Commun* **8**: 1174.
- 855 **Garcia-Mata C, Lamattina L** (2013) Gasotransmitters are emerging as new guard cell  
856 signaling molecules and regulators of leaf gas exchange. *Plant Sci* **201-202**: 66-  
857 73.
- 858 **Gotor C, Garcia I, Crespo JL, Romero LC** (2013) Sulfide as a signaling molecule in  
859 autophagy. *Autophagy* **9**: 609-611.
- 860 **Gotor C, Laureano-Marin AM, Moreno I, Aroca A, Garcia I, Romero LC** (2015) Signaling  
861 in the plant cytosol: cysteine or sulfide? *Amino Acids* **47**: 2155-2164.
- 862 **Gotor C, Laureano-Marín AM, Arenas-Alfonseca L, Moreno I, Aroca Á, García I,**  
863 **Romero LC.** (2017). Advances in Plant Sulfur Metabolism and Signaling. In  
864 *Progress in Botany Vol. 78*, F.M. Cánovas, U. Lüttge, and R. Matyssek, eds  
865 (Cham: Springer International Publishing), pp. 45-66.

- 866 **Gotor C, Garcia I, Aroca A, Laureano-Marin AM, Arenas-Alfonseca L, Jurado-Flores A,**  
867 **Moreno I, Romero LC** (2019) Signaling by hydrogen sulfide and cyanide through  
868 posttranslational modification. *J Exp Bot.*
- 869 **Gu L, Jung HJ, Kim BM, Xu T, Lee K, Kim YO, Kang H** (2015) A chloroplast-localized S1  
870 domain-containing protein SRRP1 plays a role in Arabidopsis seedling growth in  
871 the presence of ABA. *J Plant Physiol* **189**: 34-41.
- 872 **Guiboileau A, Avila-Ospina L, Yoshimoto K, Soulay F, Azzopardi M, Marmagne A,**  
873 **Lothier J, Masclaux-Daubresse C** (2013) Physiological and metabolic  
874 consequences of autophagy deficiency for the management of nitrogen and  
875 protein resources in Arabidopsis leaves depending on nitrate availability. *New*  
876 *Phytol* **199**: 683-694.
- 877 **Hanaoka H, Noda T, Shirano Y, Kato T, Hayashi H, Shibata D, Tabata S, Ohsumi Y**  
878 (2002) Leaf senescence and starvation-induced chlorosis are accelerated by the  
879 disruption of an Arabidopsis autophagy gene. *Plant Physiol* **129**: 1181-1193.
- 880 **Ida T, Sawa T, Ihara H, Tsuchiya Y, Watanabe Y, Kumagai Y, Suematsu M, Motohashi**  
881 **H, Fujii S, Matsunaga T, Yamamoto M, Ono K, Devarie-Baez NO, Xian M,**  
882 **Fukuto JM, Akaike T** (2014) Reactive cysteine persulfides and S-polythiolation  
883 regulate oxidative stress and redox signaling. *Proc Natl Acad Sci USA* **111**: 7606-  
884 7611.
- 885 **Jin Z, Pei Y** (2015) Physiological Implications of Hydrogen Sulfide in Plants: Pleasant  
886 Exploration behind Its Unpleasant Odour. *Oxid Med Cell Longev* **2015**: 397502.
- 887 **Jin Z, Xue S, Luo Y, Tian B, Fang H, Li H, Pei Y** (2013) Hydrogen sulfide interacting with  
888 abscisic acid in stomatal regulation responses to drought stress in Arabidopsis.  
889 *Plant Physiol Biochem* **62**: 41-46.
- 890 **Kimura H** (2015) Hydrogen sulfide and polysulfides as signaling molecules. *Proc Jpn*  
891 *Acad Ser B Phys Biol Sci* **91**: 131-159.
- 892 **Kirisako T, Ichimura Y, Okada H, Kabeya Y, Mizushima N, Yoshimori T, Ohsumi M,**  
893 **Takao T, Noda T, Ohsumi Y** (2000) The reversible modification regulates the  
894 membrane-binding state of Apg8/Aut7 essential for autophagy and the  
895 cytoplasm to vacuole targeting pathway. *J Cell Biol* **151**: 263-276.
- 896 **Klie S, Nikoloski Z** (2012) The Choice between MapMan and Gene Ontology for  
897 Automated Gene Function Prediction in Plant Science. *Front Genet* **3**: 115.
- 898 **Laureano-Marin AM, Moreno I, Romero LC, Gotor C** (2016a) Negative Regulation of  
899 Autophagy by Sulfide Is Independent of Reactive Oxygen Species. *Plant Physiol*  
900 **171**: 1378-1391.
- 901 **Laureano-Marin AM, Moreno I, Aroca Á, García I, Romero LC, Gotor C.** (2016b).  
902 Regulation of Autophagy by Hydrogen Sulfide. In *Gasotransmitters in Plants:*  
903 *The Rise of a New Paradigm in Cell Signaling*, L. Lamattina and C. García-Mata,  
904 eds (Cham: Springer International Publishing), pp. 53-75.
- 905 **Li Y, Zhang Y, Wang L, Wang P, Xue Y, Li X, Qiao X, Zhang X, Xu T, Liu G, Li P, Chen C**  
906 (2017) Autophagy impairment mediated by S-nitrosation of ATG4B leads to  
907 neurotoxicity in response to hyperglycemia. *Autophagy* **13**: 1145-1160.
- 908 **Liu Y, Bassham DC** (2012) Autophagy: pathways for self-eating in plant cells. *Annu Rev*  
909 *Plant Biol* **63**: 215-237.
- 910 **Liu Y, Xiong Y, Bassham DC** (2009) Autophagy is required for tolerance of drought and  
911 salt stress in plants. *Autophagy* **5**: 954-963.

- 912 **Marshall RS, Vierstra RD** (2018a) Autophagy: The Master of Bulk and Selective  
913 Recycling. *Annu Rev Plant Biol*.
- 914 **Marshall RS, Vierstra RD** (2018b) Autophagy: The Master of Bulk and Selective  
915 Recycling. *Annu Rev Plant Biol* **69**: 173-208.
- 916 **Masclaux-Daubresse C, Chen Q, Have M** (2017) Regulation of nutrient recycling via  
917 autophagy. *Curr Opin Plant Biol* **39**: 8-17.
- 918 **Mishanina TV, Libiad M, Banerjee R** (2015) Biogenesis of reactive sulfur species for  
919 signaling by hydrogen sulfide oxidation pathways. *Nat Chem Biol* **11**: 457-464.
- 920 **Mizushima N, Yoshimori T, Ohsumi Y** (2011) The role of Atg proteins in  
921 autophagosome formation. *Annu Rev Cell Dev Biol* **27**: 107-132.
- 922 **Mustafa AK, Gadalla MM, Sen N, Kim S, Mu W, Gazi SK, Barrow RK, Yang G, Wang R,**  
923 **Snyder SH** (2009) H<sub>2</sub>S signals through protein S-sulfhydration. *Sci Signal* **2**:  
924 ra72.
- 925 **Nair U, Yen W-L, Mari M, Cao Y, Xie Z, Baba M, Reggiori F, Klionsky DJ** (2012) A role  
926 for Atg8-PE deconjugation in autophagosome biogenesis. *Autophagy* **8**: 780-  
927 793.
- 928 **Nakatogawa H, Ishii J, Asai E, Ohsumi Y** (2012) Atg4 recycles inappropriately lipidated  
929 Atg8 to promote autophagosome biogenesis. *Autophagy* **8**: 177-186.
- 930 **Papanatsiou M, Scuffi D, Blatt MR, García-Mata C** (2015) Hydrogen Sulfide Regulates  
931 Inward-Rectifying K<sup>+</sup> Channels in Conjunction with Stomatal Closure. *Plant*  
932 *Physiol* **168**: 29-35.
- 933 **Paul BD, Snyder SH** (2012) H<sub>2</sub>S signalling through protein sulfhydration and beyond.  
934 *Nat Rev Mol Cell Biol* **13**: 499-507.
- 935 **Perez-Perez ME, Florencio FJ, Crespo JL** (2010) Inhibition of Target of Rapamycin  
936 Signaling and Stress Activate Autophagy in *Chlamydomonas reinhardtii*. *Plant*  
937 *Physiol* **152**: 1874-1888.
- 938 **Perez-Perez ME, Lemaire SD, Crespo JL** (2016) Control of Autophagy in  
939 *Chlamydomonas* Is Mediated through Redox-Dependent Inactivation of the  
940 ATG4 Protease. *Plant Physiol* **172**: 2219-2234.
- 941 **Perez-Perez ME, Zaffagnini M, Marchand CH, Crespo JL, Lemaire SD** (2014) The yeast  
942 autophagy protease Atg4 is regulated by thioredoxin. *Autophagy* **10**: 1953-  
943 1964.
- 944 **Pérez-Pérez ME, Lemaire SD, Crespo JL** (2012) Reactive oxygen species and autophagy  
945 in plants and algae. *Plant Physiol* **160**: 156-164.
- 946 **Phillips AR, Suttangkakul A, Vierstra RD** (2008) The ATG12-conjugating enzyme ATG10  
947 Is essential for autophagic vesicle formation in *Arabidopsis thaliana*. *Genetics*  
948 **178**: 1339-1353.
- 949 **Romero LC, Garcia I, Gotor C** (2013) L-Cysteine Desulfhydrase 1 modulates the  
950 generation of the signaling molecule sulfide in plant cytosol. *Plant Signal Behav*  
951 **8**: e24007.
- 952 **Sali A, Blundell TL** (1993) Comparative protein modelling by satisfaction of spatial  
953 restraints. *J Mol Biol* **234**: 779-815.
- 954 **Sato A, Sato Y, Fukao Y, Fujiwara M, Umezawa T, Shinozaki K, Hibi T, Taniguchi M,**  
955 **Miyake H, Goto DB, Uozumi N** (2009) Threonine at position 306 of the KAT1  
956 potassium channel is essential for channel activity and is a target site for ABA-  
957 activated SnRK2/OST1/SnRK2.6 protein kinase. *Biochem J* **424**: 439-448.

- 958 **Satoo K, Noda NN, Kumeta H, Fujioka Y, Mizushima N, Ohsumi Y, Inagaki F** (2009) The  
959 structure of Atg4B-LC3 complex reveals the mechanism of LC3 processing and  
960 delipidation during autophagy. *EMBO J* **28**: 1341-1350.
- 961 **Scherz-Shouval R, Shvets E, Fass E, Shorer H, Gil L, Elazar Z** (2007) Reactive oxygen  
962 species are essential for autophagy and specifically regulate the activity of  
963 Atg4. *EMBO J* **26**: 1749-1760.
- 964 **Scuffi D, Álvarez C, Laspina N, Gotor C, Lamattina L, García-Mata C** (2014) Hydrogen  
965 Sulfide Generated by L-Cysteine Desulfhydrase Acts Upstream of Nitric Oxide to  
966 Modulate Abscisic Acid-Dependent Stomatal Closure. *Plant Physiol* **166**: 2065-  
967 2076.
- 968 **Scuffi D, Nietzel T, Di Fino LM, Meyer AJ, Lamattina L, Schwarzländer M, Laxalt AM,**  
969 **García-Mata C** (2018) Hydrogen Sulfide Increases Production of NADPH  
970 Oxidase-Dependent Hydrogen Peroxide and Phospholipase D-Derived  
971 Phosphatidic Acid in Guard Cell Signaling. *Plant Physiol* **176**: 2532.
- 972 **Sen N** (2017) Functional and Molecular Insights of Hydrogen Sulfide Signaling and  
973 Protein Sulfhydration. *J Mol Biol* **429**: 543-561.
- 974 **Seo E, Woo J, Park E, Bertolani SJ, Siegel JB, Choi D, Dinesh-Kumar SP** (2016)  
975 Comparative analyses of ubiquitin-like ATG8 and cysteine protease ATG4  
976 autophagy genes in the plant lineage and cross-kingdom processing of ATG8 by  
977 ATG4. *Autophagy* **12**: 2054-2068.
- 978 **Shen J, Zhang J, Zhou M, Zhou H, Cui B, Gotor C, Romero LC, Fu L, Yang J, Foyer CH,**  
979 **Pan Q, Shen W, Xie Y** (2020) Persulfidation-based Modification of Cysteine  
980 Desulfhydrase and the NADPH Oxidase RBOHD Controls Guard Cell Abscisic  
981 Acid Signaling. *Plant Cell* **32**: 1000-1017.
- 982 **Shu CW, Drag M, Bekes M, Zhai D, Salvesen GS, Reed JC** (2010) Synthetic substrates  
983 for measuring activity of autophagy proteases: autophagins (Atg4). *Autophagy*  
984 **6**: 936-947.
- 985 **Soto-Burgos J, Zhuang X, Jiang L, Bassham DC** (2018) Dynamics of Autophagosome  
986 Formation. *Plant Physiol* **176**: 219-229.
- 987 **Sugawara K, Suzuki NN, Fujioka Y, Mizushima N, Ohsumi Y, Inagaki F** (2005) Structural  
988 basis for the specificity and catalysis of human Atg4B responsible for  
989 mammalian autophagy. *J Biol Chem* **280**: 40058-40065.
- 990 **Thimm O, Blasing O, Gibon Y, Nagel A, Meyer S, Kruger P, Selbig J, Muller LA, Rhee**  
991 **SY, Stitt M** (2004) MAPMAN: a user-driven tool to display genomics data sets  
992 onto diagrams of metabolic pathways and other biological processes. *Plant J*  
993 **37**: 914-939.
- 994 **Toohey JI** (2011) Sulfur signaling: is the agent sulfide or sulfane? *Anal Biochem* **413**: 1-  
995 7.
- 996 **Ustun S, Hafren A, Hofius D** (2017) Autophagy as a mediator of life and death in  
997 plants. *Curr Opin Plant Biol* **40**: 122-130.
- 998 **Vanhee C, Batoko H** (2011) Autophagy involvement in responses to abscisic acid by  
999 plant cells. *Autophagy* **7**: 655-656.
- 1000 **Vanhee C, Zapotoczny G, Masquelier D, Ghislain M, Batoko H** (2011) The Arabidopsis  
1001 Multistress Regulator TSPO Is a Heme Binding Membrane Protein and a  
1002 Potential Scavenger of Porphyrins via an Autophagy-Dependent Degradation  
1003 Mechanism. *The Plant Cell* **23**: 785-805.

1004 **Vitvitsky V, Miljkovic JL, Bostelaar T, Adhikari B, Yadav PK, Steiger AK, Torregrossa R,**  
1005 **Pluth MD, Whiteman M, Banerjee R, Filipovic MR** (2018) Cytochrome c  
1006 Reduction by H<sub>2</sub>S Potentiates Sulfide Signaling. *ACS Chem Biol* **13**: 2300-2307.  
1007 **Wang M, Tang W, Zhu YZ** (2017) An Update on AMPK in Hydrogen Sulfide  
1008 Pharmacology. *Front Pharmacol* **8**: 810.  
1009 **Wang P, Zhao Y, Li Z, Hsu CC, Liu X, Fu L, Hou YJ, Du Y, Xie S, Zhang C, Gao J, Cao M,**  
1010 **Huang X, Zhu Y, Tang K, Wang X, Tao WA, Xiong Y, Zhu JK** (2018) Reciprocal  
1011 Regulation of the TOR Kinase and ABA Receptor Balances Plant Growth and  
1012 Stress Response. *Mol Cell* **69**: 100-112 e106.  
1013 **Wedmann R, Onderka C, Wei S, Szijarto IA, Miljkovic JL, Mitrovic A, Lange M, Savitsky**  
1014 **S, Yadav PK, Torregrossa R, Harrer EG, Harrer T, Ishii I, Gollasch M, Wood ME,**  
1015 **Galardon E, Xian M, Whiteman M, Banerjee R, Filipovic MR** (2016) Improved  
1016 tag-switch method reveals that thioredoxin acts as depersulfidase and controls  
1017 the intracellular levels of protein persulfidation. *Chem Sci* **7**: 3414-3426.  
1018 **Woo J, Park E, Dinesh-Kumar SP** (2014) Differential processing of Arabidopsis  
1019 ubiquitin-like Atg8 autophagy proteins by Atg4 cysteine proteases. *Proc Natl*  
1020 *Acad Sci U S A* **111**: 863-868.  
1021 **Wu D, Wang H, Teng T, Duan S, Ji A, Li Y** (2018) Hydrogen sulfide and autophagy: A  
1022 double edged sword. *Pharmacol Res* **131**: 120-127.  
1023 **Xiong Y, Contento AL, Bassham DC** (2005) AtATG18a is required for the formation of  
1024 autophagosomes during nutrient stress and senescence in Arabidopsis thaliana.  
1025 *Plant J* **42**: 535-546.  
1026 **Xiong Y, Contento AL, Nguyen PQ, Bassham DC** (2007) Degradation of oxidized  
1027 proteins by autophagy during oxidative stress in Arabidopsis. *Plant Physiol* **143**:  
1028 291-299.  
1029 **Yoshimoto K, Hanaoka H, Sato S, Kato T, Tabata S, Noda T, Ohsumi Y** (2004)  
1030 Processing of ATG8s, ubiquitin-like proteins, and their deconjugation by ATG4s  
1031 are essential for plant autophagy. *Plant Cell* **16**: 2967-2983.  
1032 **Yu Z-Q, Ni T, Hong B, Wang H-Y, Jiang F-J, Zou S, Chen Y, Zheng X-L, Klionsky DJ, Liang**  
1033 **Y** (2012) Dual roles of Atg8- PE deconjugation by Atg4 in autophagy. *Autophagy*  
1034 **8**: 883-892.  
1035 **Zaffagnini M, Fermani S, Marchand CH, Costa A, Sparla F, Rouhier N, Geigenberger P,**  
1036 **Lemaire SD, Trost P** (2019) Redox Homeostasis in Photosynthetic Organisms:  
1037 Novel and Established Thiol-Based Molecular Mechanisms. *Antioxid Redox*  
1038 *Signal* **31**: 155-210.  
1039 **Zheng X, Yang Z, Gu Q, Xia F, Fu Y, Liu P, Yin XM, Li M** (2020) The protease activity of  
1040 human ATG4B is regulated by reversible oxidative modification. *Autophagy*: 1-  
1041 13.  
1042  
1043  
1044  
1045

1046 **Figure Legends**

1047

1048 **Figure 1.** Proteomic analysis of protein persulfidation in response to ABA in mesophyll  
1049 cells.

1050 (A) Workflow of ABA leaf treatments followed by tag-switch protein labeling with CN-  
1051 biotin, protein purification, and quantitative SWATH analysis of eluted proteins.

1052 (B) PCA representation plot of the 18 samples after SWATH analysis. Score for PC1  
1053 (70 %) versus PC2 (9.9%), Pareto scaling.

1054 (C) Level of persulfidated ATG4a after ABA treatments. Values represent the mean  
1055 peak areas of extracted ion chromatogram of identified ATG4a peptides. \*,  $p < 0.05$ .

1056

1057 **Figure 2.** Effect of sulfide on autophagy induced by ABA treatment.

1058 (A) Immunoblot analysis of GFP-ATG8e fusion protein. One-week-old seedlings  
1059 expressing GFP-ATG8e fusion protein were transferred to liquid MS media and were  
1060 not treated (control) or treated with 50  $\mu$ M ABA for 3 and 6 h and then 200  $\mu$ M NaHS  
1061 for 1 h. Total protein extracts were prepared and subjected to SDS-PAGE and  
1062 immunoblot analysis with anti-GFP antibodies. Anti-tubulin antibodies were used as the  
1063 protein-loading control.

1064 (B) Quantification of the free GFP/GFP-ATG8 ratio. For each condition, the levels of  
1065 free GFP and GFP-ATG8e fusion protein were quantified in a less exposed blot shown  
1066 in Supplemental Figure 6. The value of 100% was assigned to the free GFP/GFP-ATG8  
1067 ratio of the control sample. Data are from three independent experiments and evaluated  
1068 by two-factor ANOVA. Same letters indicate no significant differences.  $P < 0.05$ .

1069

1070 **Figure 3.** Persulfidation of Arabidopsis AtATG4a.

1071 (A) Immunoblot analysis of persulfidated AtATG4a. Purified recombinant AtATG4a  
1072 was treated in the absence (-) or in the presence of 50 mM DTT (+) for 30 min at 4°C,  
1073 dialyzed, and subjected to the tag-switch labeling as described in the Methods. Then,  
1074 the proteins were subjected to immunoblot analysis using anti-biotin antibodies. Sypro  
1075 Ruby fluorescent staining is shown as the protein loading control.

1076 (B) Analysis of AtATG4a using mass spectrometry. LC-MS/MS analysis of a tryptic  
1077 peptide of AtATG4a containing Cys170. The table inside the spectrum contains the  
1078 predicted ion types for the modified peptide, and the ions detected in the spectrum are  
1079 highlighted in red.

1080 (C) AtATG4a protein sequence identified with 97% coverage. The peptide containing  
1081 persulfidated Cys170 is highlighted in yellow and all the Cys residues are red.

1082

1083 **Figure 4.** Arabidopsis ATG4a cleaves Chlamydomonas ATG8.

1084 ATG4 activity of the recombinant AtATG4a was assayed by monitoring the cleavage of  
1085 CrATG8 from the unprocessed (CrATG8) to processed (pCrATG8) forms (indicated by  
1086 arrowheads) using SDS-PAGE followed by Coomassie Blue staining and quantification  
1087 of protein band intensities. The ATG4 activity (relative units) was determined as the  
1088 ratio of the band intensity of the processed CrATG8 to the sum of the intensities of the  
1089 unprocessed and processed CrATG8. Activity value of 1 corresponds to the maximum.  
1090 Processed pCrATG8 (lane 1) and unprocessed CrATG8 (lane 2) were loaded as  
1091 controls. Representative images are shown. Data are from three independent  
1092 experiments and evaluated by two-factor ANOVA. Same letters indicate no significant  
1093 differences.  $P < 0.05$ .

1094 (A) Effect of incubation time. AtATG4a was incubated with CrATG8 in the absence or  
1095 in the presence of 10 mM DTT for the indicated times.

1096 (B) Effect of DTT concentration. AtATG4a was incubated with CrATG8 in the absence  
1097 or in the presence of increasing concentrations of DTT for 4 h.

1098 (C) Effect of TCEP concentration. AtATG4a was incubated with CrATG8 in the  
1099 absence or in the presence of increasing concentrations of TCEP for 4 h.

1100

1101 **Figure 5.** Effect of NaHS on AtATG4a enzyme activity.

1102 (A) AtATG4a was incubated with 0.5 mM TCEP for 2 h and treated in the absence or in  
1103 the presence of indicated concentrations of NaHS for 1 h. Then, CrATG8 was added to  
1104 the incubation mixture, and ATG4 activity was monitored after 4 h using Coomassie-  
1105 stained gels as described in the Methods. All procedures were performed at 25°C. Lane  
1106 1 and 2, unprocessed and processed CrATG8, respectively. Lane 3, AtATG4a incubated  
1107 with CrATG8 in the absence of TCEP and of NaHS. Lanes 4-8, TCEP-pretreated  
1108 reduced AtATG4a incubated with CrATG8 in the presence of increasing concentrations  
1109 of NaHS (from 0 to 1 mM). A representative image is shown.

1110 (B) Quantification of ATG4 activity (relative units) determined as the ratio of the band  
1111 intensity of the processed CrATG8 to the sum of the intensities of the unprocessed and  
1112 processed CrATG8. A value of 1 corresponds to AtATG4a in the absence of NaHS  
1113 (lane 4).

1114 (C) Quantification of the protein band intensity corresponding to the monomeric  
1115 AtATG4a form marked by a rectangle in A. A value of 100% corresponds to AtATG4a  
1116 in the absence of NaHS (lane 4).

1117 Data are from three independent experiments and evaluated by two-factor ANOVA.  
1118 Same letters indicate no significant differences.  $P < 0.05$ .

1119

1120

1121 **Figure 6.** Effect of polysulfides on AtATG4a enzyme activity.

1122 (A) AtATG4a was incubated with 0.5 mM TCEP for 2 h and subsequently treated in the  
1123 absence or in the presence of indicated concentrations of  $\text{Na}_2\text{S}_4$  for 1 h. Then, CrATG8  
1124 was added to the incubation mixture, and ATG4 activity was monitored after 4 h using  
1125 Coomassie-stained gels as described in Methods. All procedures were performed at 25  
1126 °C. A representative image is shown.

1127 (B) Quantification of ATG4 activity (relative units) determined as the ratio of the band  
1128 intensity of the processed CrATG8 to the sum of the intensities of the unprocessed and  
1129 processed CrATG8. A value of 1 corresponds to AtATG4a treated in the absence of  
1130  $\text{Na}_2\text{S}_4$  (lane 1).

1131 (C) Quantification of the protein band intensity corresponding to the monomeric  
1132 AtATG4a form marked by a rectangle in A. A value of 100% corresponds to AtATG4a  
1133 treated in the absence of  $\text{Na}_2\text{S}_4$  (lane 1).

1134 (D) Reversibility of the effect. AtATG4a was incubated with 0.25 mM TCEP for 2 h  
1135 (lane 1) and treated with 100  $\mu\text{M}$   $\text{Na}_2\text{S}_4$  for 1 h (lane 2) and 1 mM TCEP for 1 h (lane  
1136 3). ATG4 activity was monitored using Coomassie-stained gels. The experiment was  
1137 performed at least three times and a representative image used for the quantification of  
1138 the activity is shown.

1139 Data are from three independent experiments and evaluated by two-factor ANOVA.  
1140 Same letters indicate no significant differences.  $P < 0.05$ .

1141

1142

1143 **Figure 7.** Predicted structure of the AtATG4a-AtATG8a complex.

1144 (A) 3D modelling of the AtATG4a-AtATG8a complex based on the structure of the  
1145 HsAtg4B-LC3 protein complex (PDB ID: 2Z0E). The AtATG8 protein sequence  
1146 (Q8LEM4 in UniProtKB) corresponds to the splice variant 1. Surface representation of  
1147 the protein complex and the equivalent residues surrounding the catalytic cavity

1148 Cys170, Trp192, Asp364, and His366 in AtATG4a (red) and Phe116, Gly117, Thr120,  
1149 and Ala122 in AtATG8a (blue) are shown in the structural models.

1150 **(B)** Zoomed view of the putative conformation of the active site showing the spheres  
1151 corresponding to the position and distance (Å) of catalytic residues Cys170, Trp192,  
1152 Asp364, and His366 in AtATG4a.

1153

1154 **Figure 8.** Cleavage and conjugation of Chlamydomonas ATG8 by Arabidopsis  
1155 proteins.

1156 **(A)** ATG4 proteolytic activity in wild-type Arabidopsis leaves. Arabidopsis protein  
1157 extracts prepared from leaves of wild-type seedlings grown for 11 days on MS medium  
1158 were incubated with CrATG8 or site-directed mutant G120A proteins at 25°C for the  
1159 indicated times, and ATG4 activity was monitored as the cleavage of the ATG8 forms  
1160 to the processed (pCrATG8) forms by immunoblotting analysis with anti-CrATG8.  
1161 Processed pCrATG8 (lane 1), unprocessed CrATG8 (lane 2), and site-directed mutant  
1162 G120A (lane 6) were loaded as controls.

1163 **(B)** ATG4 proteolytic activity in the Arabidopsis *atg4ab* mutant. Arabidopsis protein  
1164 extracts were prepared from the leaves of wild-type and *atg4ab* double mutant seedlings  
1165 grown for 7 days on the MS medium and transferred to the same medium (+N) or to a  
1166 nitrogen-deficient medium (-N) for additional 4 days. The protein extracts were  
1167 incubated with CrATG8 at 25°C, and ATG4 activity was monitored after 0, 0.5, or 2 h  
1168 as indicated by immunoblotting analysis with anti-CrATG8.

1169 The arrowheads show the unprocessed CrATG8 and processed pCrATG8 protein bands,  
1170 and the asterisks indicate faster-mobility protein bands. Ponceau staining is shown as  
1171 the protein loading control of the Arabidopsis extract.

1172

1173 **Figure 9.** Sulfide inhibits the endogenous proteolytic activity of Arabidopsis ATG4.

1174 **(A)** Effect of polysulfides on endogenous enzyme activity of Arabidopsis ATG4.  
1175 Arabidopsis protein extracts (Ex) were prepared from the leaves of seedlings grown for  
1176 11 days on the MS medium. The extracts were treated in the absence (un-Ex) and in the  
1177 presence of 200 μM Na<sub>2</sub>S<sub>4</sub> (Na<sub>2</sub>S<sub>4</sub>-Ex), or 20 mM iodoacetamide (IAM-Ex) for 30 min,  
1178 or in the presence of 200 μM Na<sub>2</sub>S<sub>4</sub> for 30 min and 1 mM TCEP for 30 min (Na<sub>2</sub>S<sub>4</sub>-Ex  
1179 + TCEP). Then, CrATG8 was added to the incubation mixture, and ATG4 proteolytic  
1180 activity was monitored. Lane 1, unprocessed CrATG8.

1181 (B) Sulfide reverts the endogenous enzyme activity of Arabidopsis ATG4 under  
1182 autophagy-induced conditions. Arabidopsis protein extracts were prepared from the  
1183 leaves of seedlings grown for 7 days on the MS medium and transferred to the same  
1184 medium (+N) or to a nitrogen-deficient medium (-N) (left panel); or transferred to the  
1185 same medium (-mannitol) or to same medium containing 300 mM mannitol (+mannitol)  
1186 (right panel) for additional 4 days. The extracts were treated in the absence (un-Ex) or  
1187 in the presence of 200  $\mu$ M  $\text{Na}_2\text{S}_4$  for 30 min ( $\text{Na}_2\text{S}_4$ -EX); CrATG8 was added to the  
1188 incubation mixture and ATG4 activity was monitored. Lane 1, processed pCrATG8 and  
1189 lane 2, unprocessed CrATG8.  
1190 The ATG4 activity was monitored at the indicated times by immunoblotting analysis  
1191 with anti-CrATG8. All procedures were performed at 25°C. Ponceau staining is shown  
1192 as the protein loading control.

1193

1194 **Figure 10.** Graphical model of ABA-triggered induction of autophagy mediated by  
1195 posttranslational modification of ATG4. Under basal conditions, intracellular sulfide  
1196 maintains high levels of persulfidation of the ATG4 pool, which inhibits the proteolytic  
1197 activity of the enzyme for ATG8 C-terminal processing. An increase in the intracellular  
1198 level of ABA transiently decreases the level of persulfidation of the ATG4 population  
1199 activating the protease activity of the enzyme and the processing of ATG8 that can be  
1200 further lipidated to progress autophagy. Yellow circles represent ATG8 protein with or  
1201 without the processed C-terminus (represented as X). Blue semicircles represent  
1202 persulfidated ATG4 at the thiol group of Cys170 residue. Blue Pacman symbols  
1203 represent ATG4 with reduced thiol group of Cys170 residue. The conjugation process  
1204 of ATG8 with phosphatidylethanolamine (PE) and autophagosome initiation and  
1205 closure are also shown.

1206

1207

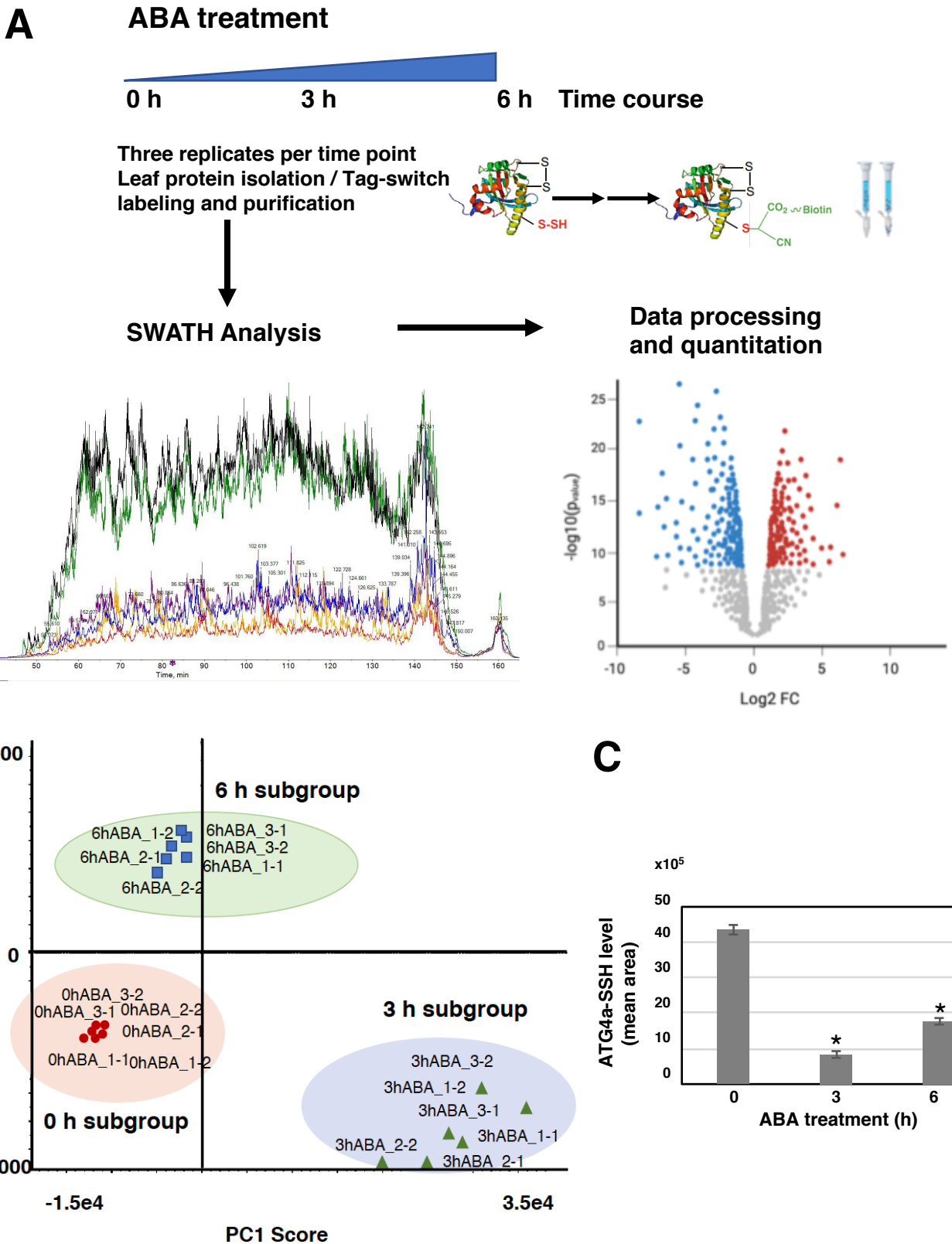


**Figure 1.** Proteomic analysis of protein persulfidation in response to ABA in mesophyll cells.

**(A)** Workflow of ABA leaf treatments followed by tag-switch protein labeling with CN-biotin, protein purification, and quantitative SWATH analysis of eluted proteins.

**(B)** PCA representation plot of the 18 samples after SWATH analysis. Score for PC1 (70 %) versus PC2 (9.9%), Pareto scaling.

**(C)** Level of persulfidated ATG4a after ABA treatments. Values represent the mean peak areas of extracted ion chromatogram of identified ATG4a peptides. \*,  $p < 0.05$

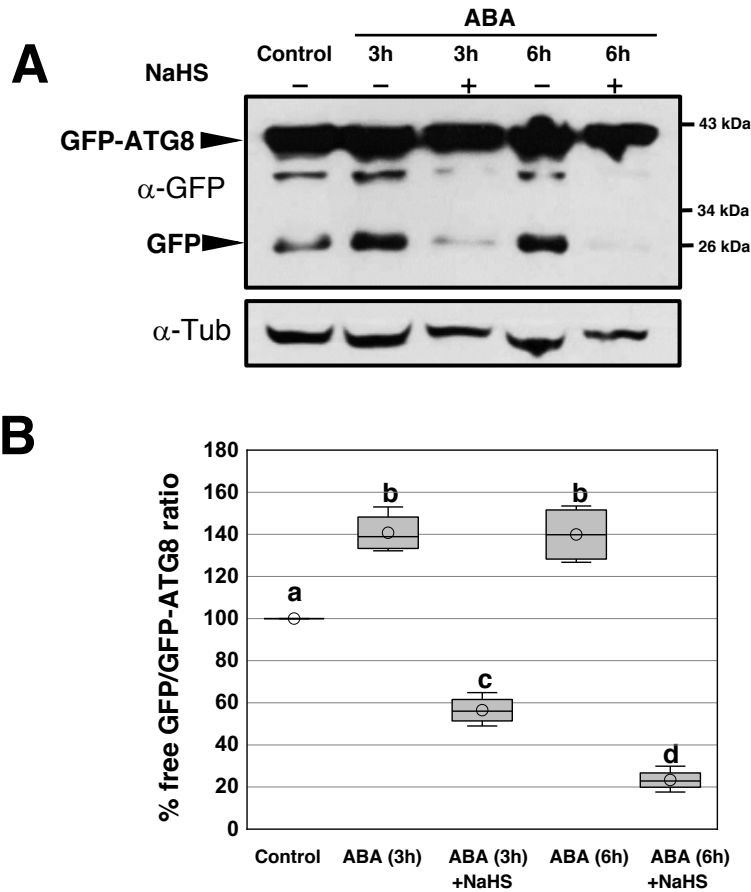


**Figure 2.** Effect of sulfide on autophagy induced by ABA treatment.

**(A)** Immunoblot analysis of GFP-ATG8e fusion protein. One-week-old seedlings expressing GFP-ATG8e fusion protein were transferred to liquid MS media and were not treated (control) or treated with 50  $\mu$ M ABA for 3 and 6 h and then 200  $\mu$ M NaHS for 1 h. Total protein extracts were prepared and subjected to SDS-PAGE and immunoblot analysis with anti-GFP antibodies. Anti-tubulin antibodies were used as the protein-loading control.

**(B)** Quantification of the free GFP/GFP-ATG8 ratio. For each condition, the levels of free GFP and GFP-ATG8e fusion protein were quantified in a less exposed blot shown in Supplemental Figure 6. The value of 100% was assigned to the free GFP/GFP-ATG8 ratio of the control sample. Data are from three independent experiments and evaluated by two-factor ANOVA. Same letters indicate no significant differences.  $P < 0.05$ .

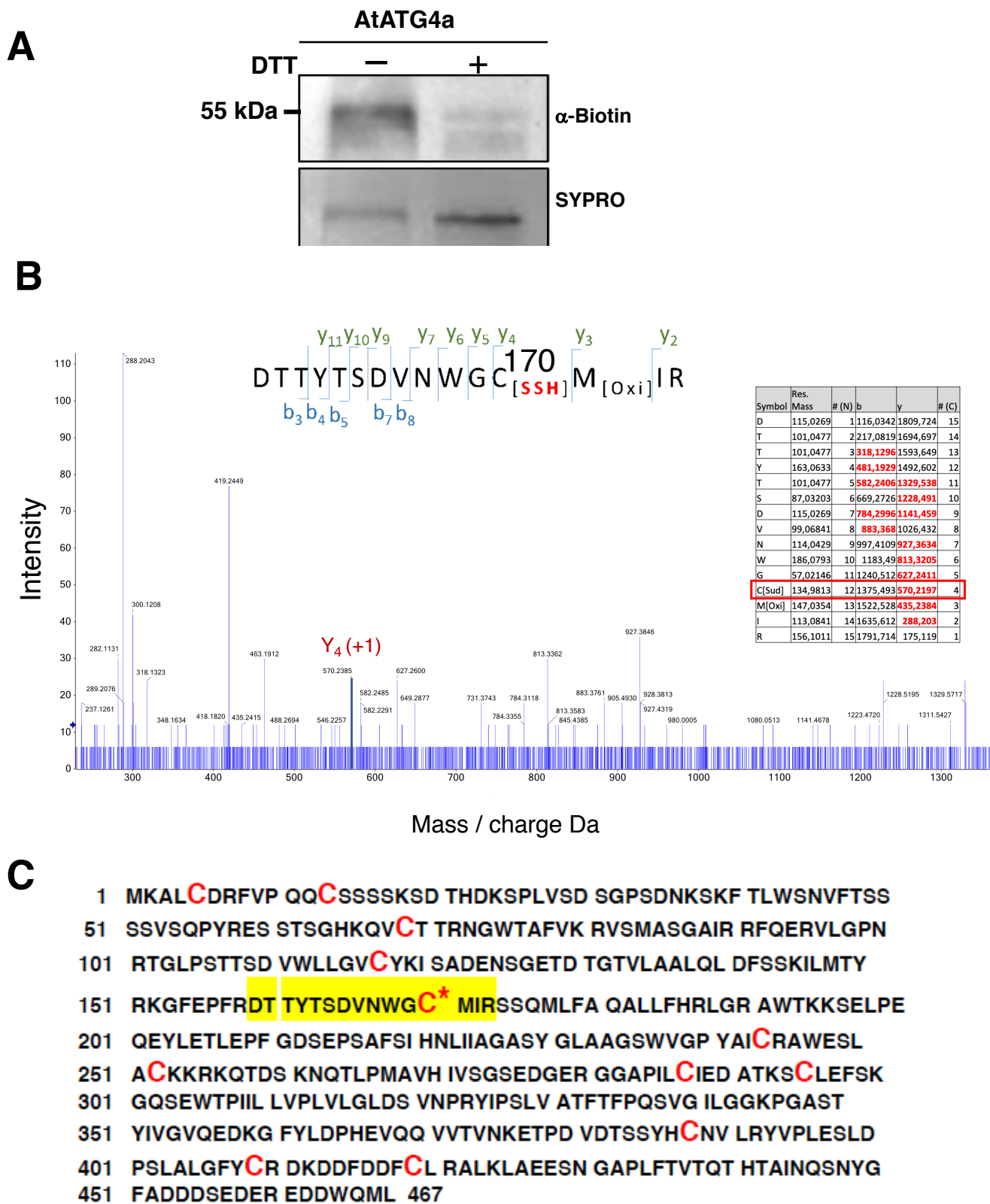


**Figure 3.** Persulfidation of Arabidopsis AtATG4a

**(A)** Immunoblot analysis of persulfidated AtATG4a. Purified recombinant AtATG4a was treated in the absence (–) or in the presence of 50 mM DTT (+) for 30 min at 4°C, dialyzed, and subjected to the tag-switch labeling as described in the Methods. Then, the proteins were subjected to immunoblot analysis using anti-biotin antibodies. Sypro Ruby fluorescent staining is shown as the protein loading control.

**(B)** Analysis of AtATG4a using mass spectrometry. LC-MS/MS analysis of a tryptic peptide of AtATG4a containing Cys170. The table inside the spectrum contains the predicted ion types for the modified peptide, and the ions detected in the spectrum are highlighted in red.

**(C)** AtATG4a protein sequence identified with 97% coverage. The peptide containing persulfidated Cys170 is highlighted in yellow and all the Cys residues are red.

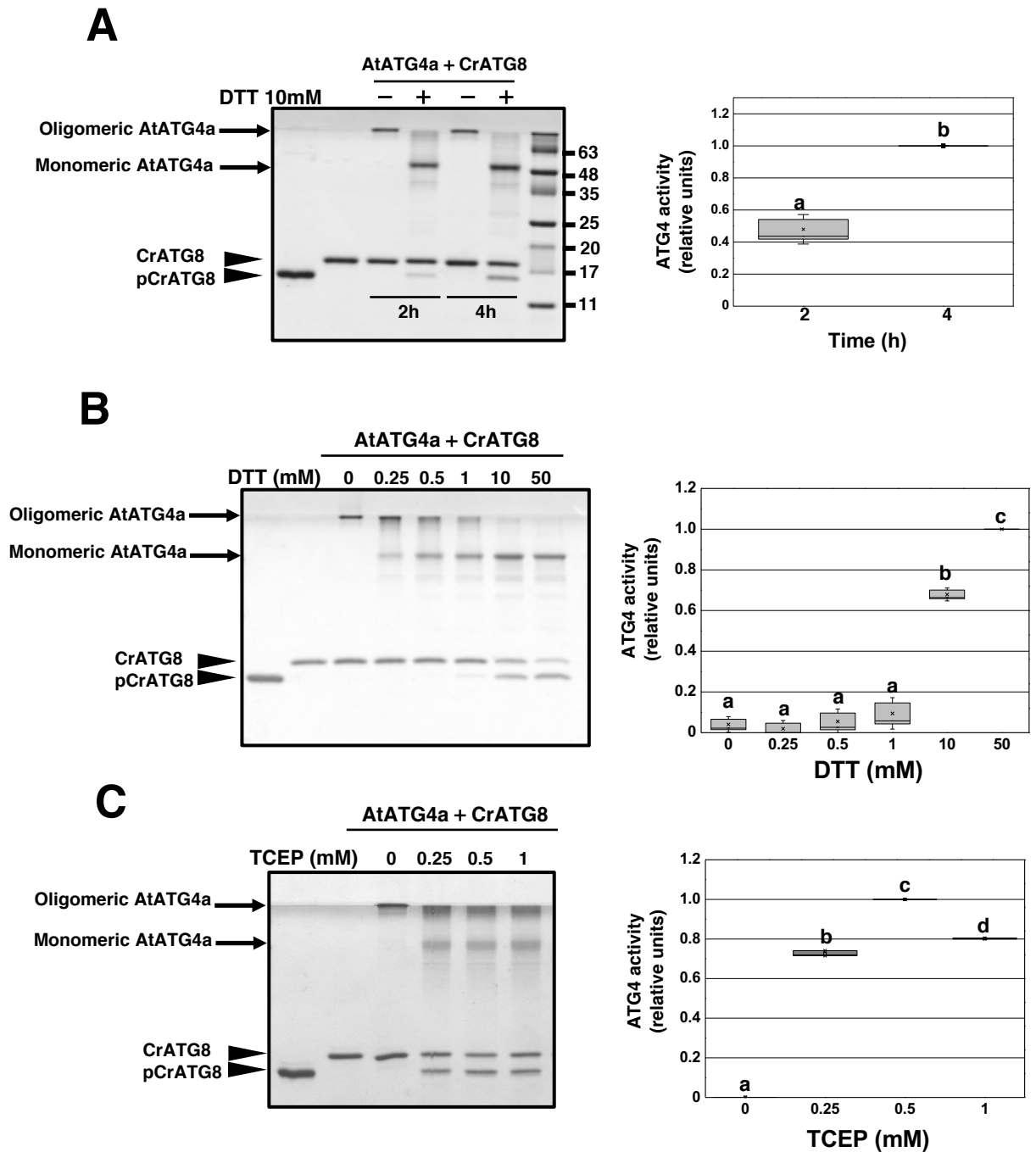


**Figure 4.** Arabidopsis ATG4a cleaves Chlamydomonas ATG8.

ATG4 activity of the recombinant AtATG4a was assayed by monitoring the cleavage of CrATG8 from the unprocessed (CrATG8) to processed (pCrATG8) forms (indicated by arrowheads) using SDS-PAGE followed by Coomassie Blue staining and quantification of protein band intensities. The ATG4 activity (relative units) was determined as the ratio of the band intensity of the processed CrATG8 to the sum of the intensities of the unprocessed and processed CrATG8. Activity value of 1 corresponds to the maximum. Processed pCrATG8 (lane 1) and unprocessed CrATG8 (lane 2) were loaded as controls. Representative images are shown. Data are from three independent experiments and evaluated by two-factor ANOVA. Same letters indicate no significant differences.  $P < 0.05$ .

**(A)** Effect of incubation time. AtATG4a was incubated with CrATG8 in the absence or in the presence of 10 mM DTT for the indicated times.

**(B)** Effect of DTT concentration. AtATG4a was incubated with CrATG8 in the absence or in the presence of increasing concentrations of DTT for 4 h.

**(C)** Effect of TCEP concentration. AtATG4a was incubated with CrATG8 in the absence or in the presence of increasing concentrations of TCEP for 4 h.

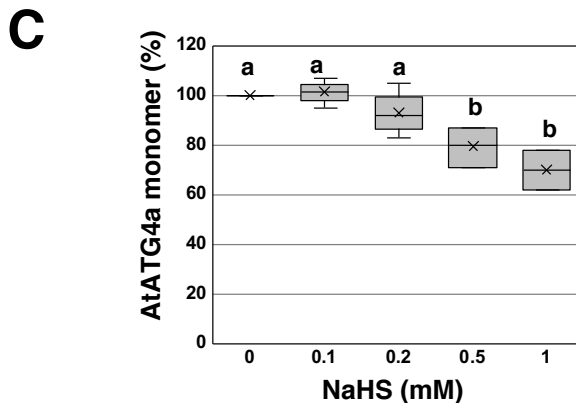
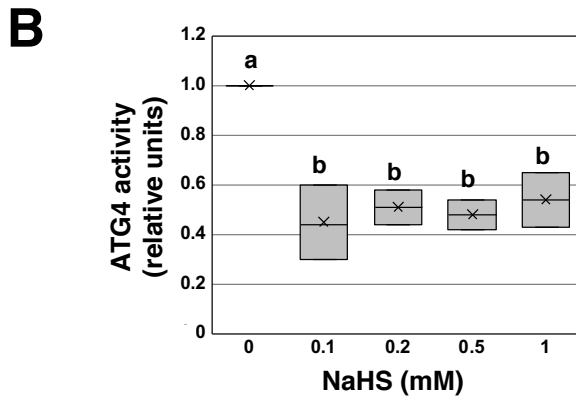
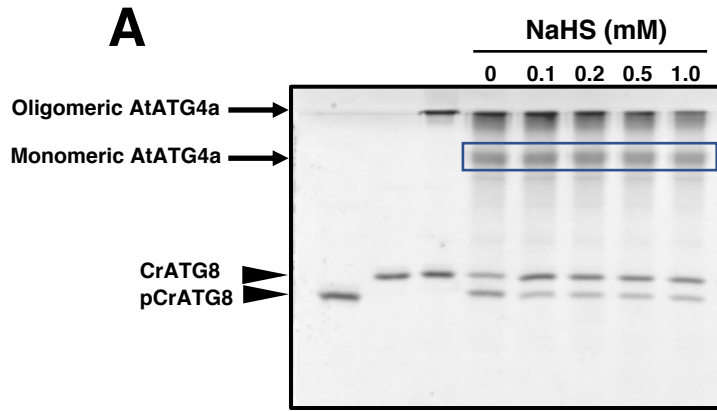


**Figure 5.** Effect of NaHS on AtATG4a enzyme activity.

**(A)** AtATG4a was incubated with 0.5 mM TCEP for 2 h and treated in the absence or the presence of indicated concentrations of NaHS for 1 h. Then, CrATG8 was added to the incubation mixture, and ATG4 activity was monitored after 4 h using Coomassie-stained gels as described in the Methods. All procedures were performed at 25°C. Lane 1 and 2, unprocessed and processed CrATG8, respectively. Lane 3, AtATG4a incubated with CrATG8 in the absence of TCEP and of NaHS. Lanes 4-8, TCEP-pretreated reduced AtATG4a incubated with CrATG8 in the presence of increasing concentrations of NaHS (from 0 to 1 mM). A representative image is shown.

**(B)** Quantification of ATG4 activity (relative units) determined as the ratio of the band intensity of the processed CrATG8 to the sum of the intensities of the unprocessed and processed CrATG8. A value of 1 corresponds to AtATG4a in the absence of NaHS (lane 4).

**(C)** Quantification of the protein band intensity corresponding to the monomeric AtATG4a form marked by a rectangle in A. A value of 100% corresponds to AtATG4a in the absence of NaHS (lane 4).

Data are from three independent experiments and evaluated by two-factor ANOVA. Same letters indicate no significant differences.  $P < 0.05$

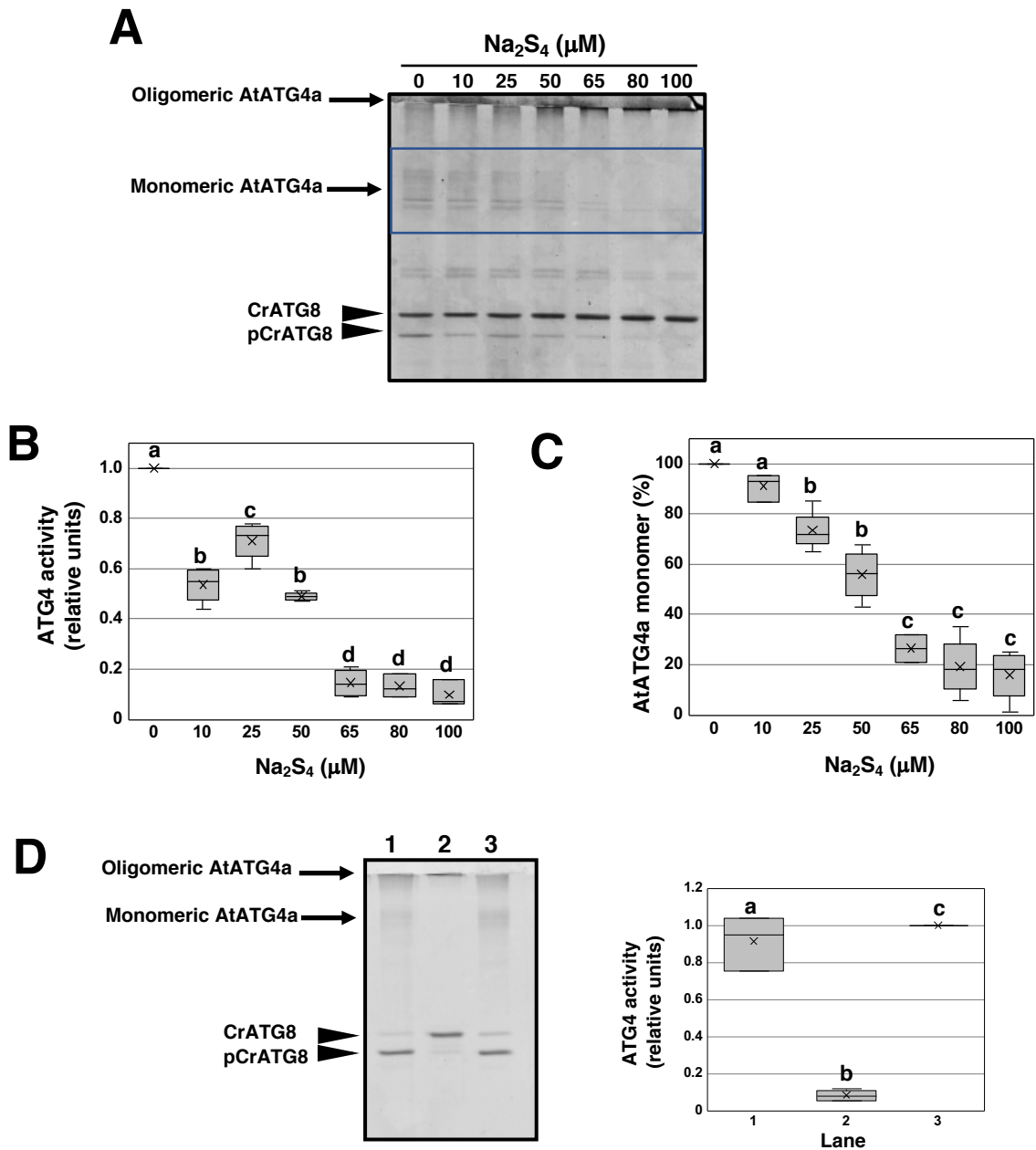


**Figure 6.** Effect of polysulfides on AtATG4a enzyme activity.

**(A)** AtATG4a was incubated with 0.5 mM TCEP for 2 h and subsequently treated in the absence or in the presence of indicated concentrations of  $\text{Na}_2\text{S}_4$  for 1 h. Then, CrATG8 was added to the incubation mixture, and ATG4 activity was monitored after 4 h using Coomassie-stained gels as described in Methods. All procedures were performed at 25°C. A representative image is shown.

**(B)** Quantification of ATG4 activity (relative units) determined as the ratio of the band intensity of the processed CrATG8 to the sum of the intensities of the unprocessed and processed CrATG8. A value of 1 corresponds to AtATG4a treated in the absence of  $\text{Na}_2\text{S}_4$  (lane 1).

**(C)** Quantification of the protein band intensity corresponding to the monomeric AtATG4a form marked by a rectangle in A. A value of 100% corresponds to AtATG4a treated in the absence of  $\text{Na}_2\text{S}_4$  (lane 1).

**(D)** Reversibility of the effect. AtATG4a was first incubated with 0.25 mM TCEP for 2 h (lane 1) and treated with 100  $\mu\text{M}$   $\text{Na}_2\text{S}_4$  for 1 h (lane 2) and 1 mM TCEP for 1 h (lane 3). ATG4 activity was monitored using Coomassie-stained gels. The experiment was performed at least three times and a representative image used for the quantification of the activity is shown.

Data are from three independent experiments and evaluated by two-factor ANOVA. Same letters indicate no significant differences.  $P < 0.05$

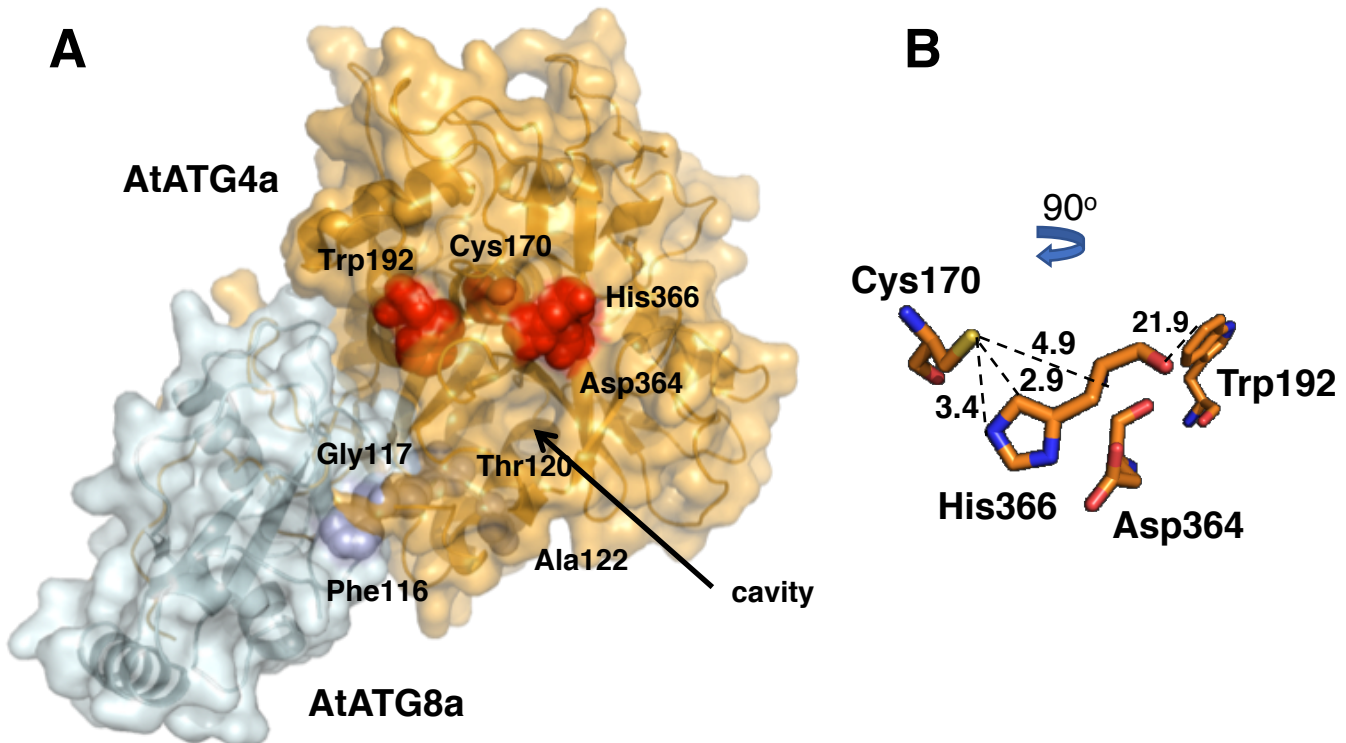


**Figure 7.** Predicted structure of the AtATG4a-AtATG8a complex.

**(A)** 3D modelling of the AtATG4a-AtATG8a complex based on the structure of the HsAtg4B-LC3 protein complex (PDB ID: 2Z0E). The AtATG8 protein sequence (Q8LEM4 in UniProtKB) corresponds to the splice variant 1. Surface representation of the protein complex and the equivalent residues surrounding the catalytic cavity Cys170, Trp192, Asp364, and His366 in AtATG4a (red) and Phe116, Gly117, Thr120, and Ala122 in AtATG8a (blue) are shown in the structural models.

**(B)** Zoomed view of the putative conformation of the active site showing the spheres corresponding to the position and distance (Å) of catalytic residues Cys170, Trp192, Asp364, and His366 in AtATG4a.

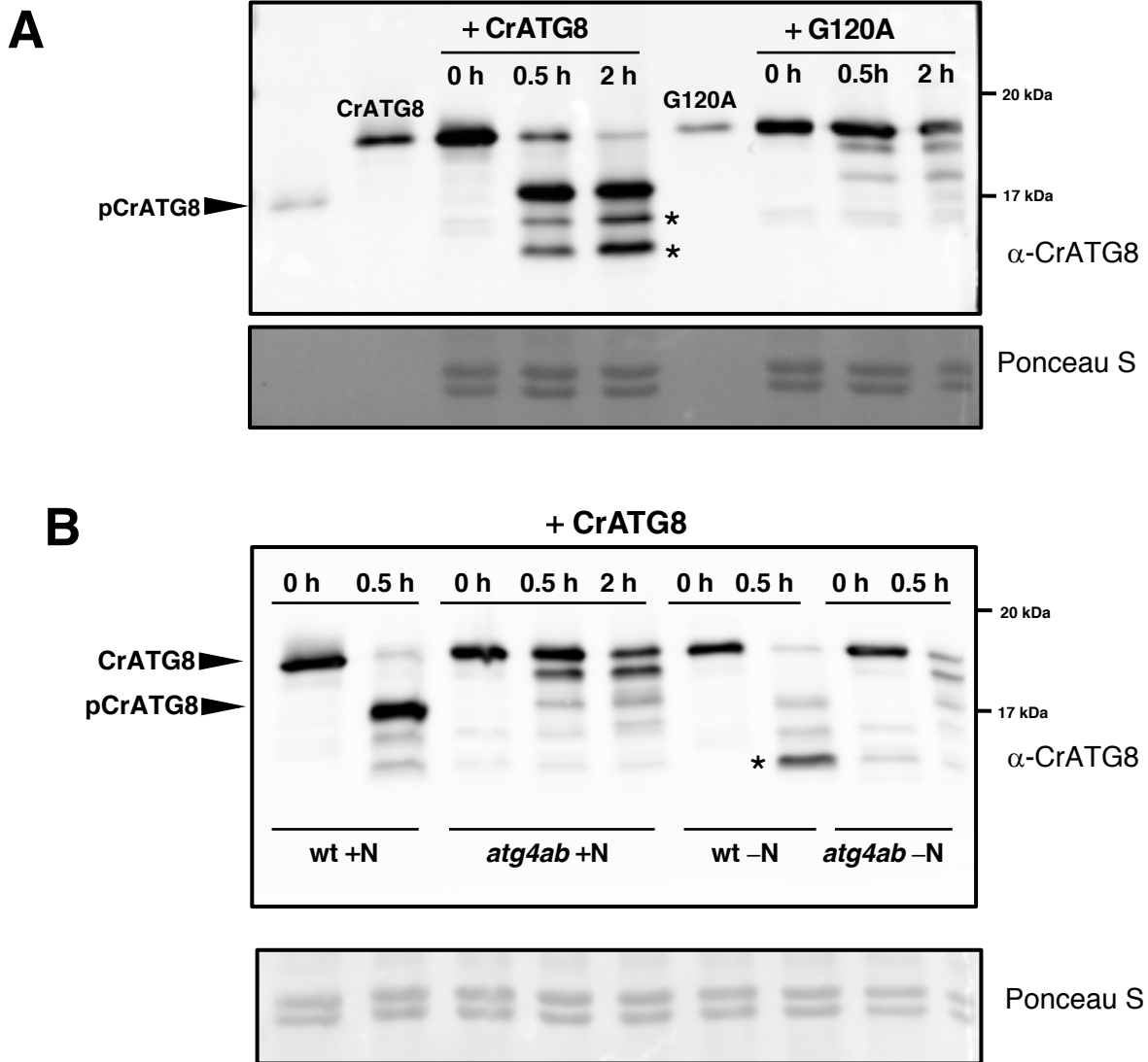


**Figure 8.** Cleavage and conjugation of Chlamydomonas ATG8 by Arabidopsis proteins.

**(A)** ATG4 proteolytic activity in wild-type Arabidopsis leaves. Arabidopsis protein extracts prepared from leaves of wild-type seedlings grown for 11 days on MS medium were incubated with CrATG8 or site-directed mutant G120A proteins at 25°C for the indicated times, and ATG4 activity was monitored as the cleavage of the ATG8 forms to the processed (pCrATG8) forms by immunoblotting analysis with anti-CrATG8. Processed pCrATG8 (lane 1), unprocessed CrATG8 (lane 2), and site-directed mutant G120A (lane 6) were loaded as controls.

**(B)** ATG4 proteolytic activity in the Arabidopsis *atg4ab* mutant. Arabidopsis protein extracts were prepared from the leaves of wild-type and *atg4ab* double mutant seedlings grown for 7 days on the MS medium and transferred to the same medium (+N) or to a nitrogen-deficient medium (-N) for additional 4 days. The protein extracts were incubated with CrATG8 at 25°C, and ATG4 activity was monitored after 0, 0.5, or 2 h, as indicated by immunoblotting analysis with anti-CrATG8.

The arrowheads show the unprocessed CrATG8 and processed pCrATG8 protein bands, and the asterisks indicate faster-mobility protein bands. Ponceau staining is shown as the protein loading control of the Arabidopsis extract.

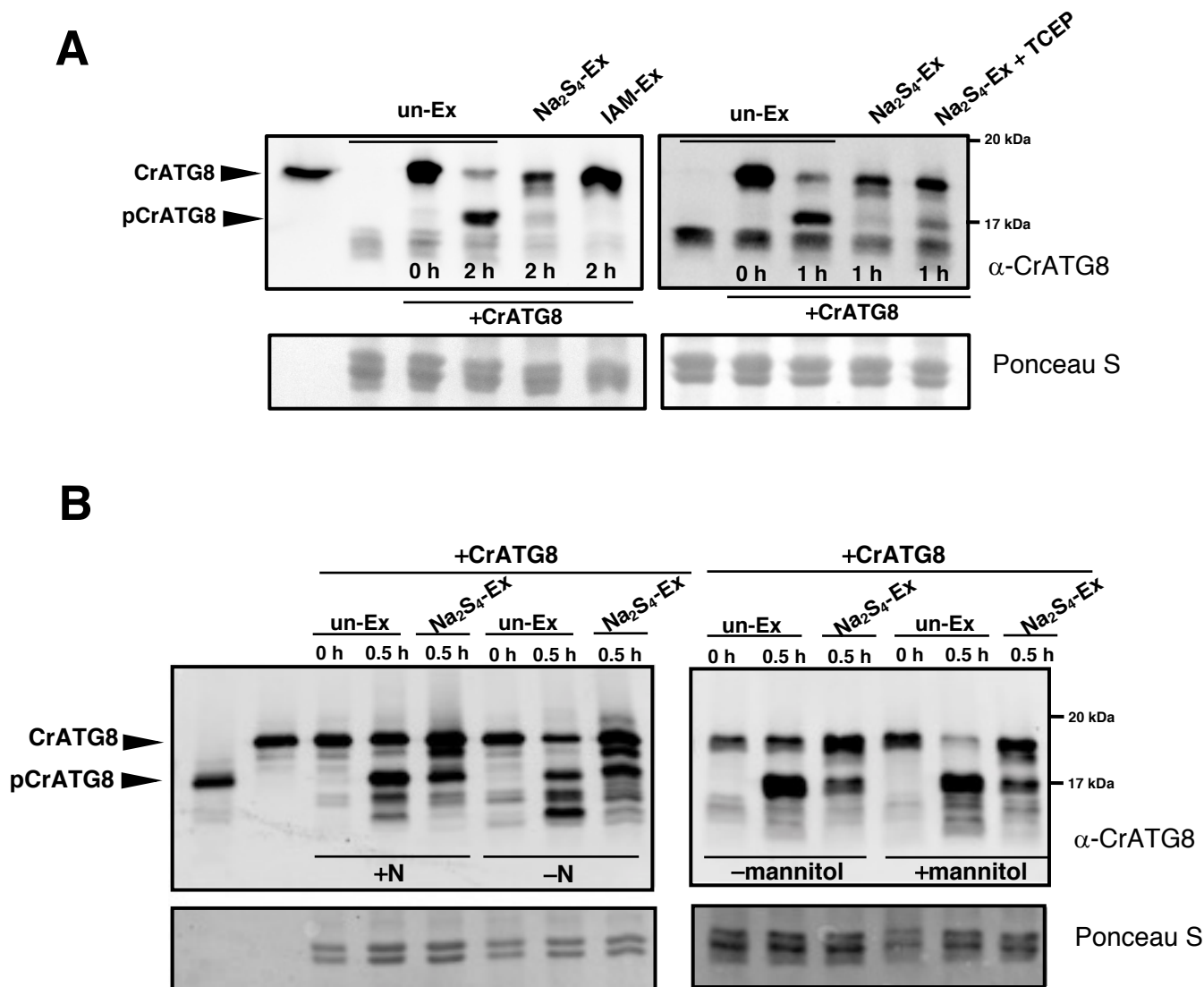


**Figure 9.** Sulfide inhibits the endogenous proteolytic activity of Arabidopsis ATG4.

**(A)** Effect of polysulfides on endogenous enzyme activity of Arabidopsis ATG4. Arabidopsis protein extracts (Ex) were prepared from the leaves of seedlings grown for 11 days on the MS medium. The extracts were treated in the absence (un-Ex) and in the presence of 200  $\mu$ M  $\text{Na}_2\text{S}_4$  ( $\text{Na}_2\text{S}_4$ -Ex), or 20 mM iodoacetamide (IAM-Ex) for 30 min, or in the presence of 200  $\mu$ M  $\text{Na}_2\text{S}_4$  for 30 min and 1 mM TCEP for 30 min ( $\text{Na}_2\text{S}_4$ -Ex + TCEP). Then, CrATG8 was added to the incubation mixture, and ATG4 proteolytic activity was monitored. Lane 1, unprocessed CrATG8.

**(B)** Sulfide reverts the endogenous enzyme activity of Arabidopsis ATG4 under autophagy-induced conditions. Arabidopsis protein extracts were prepared from the leaves of seedlings grown for 7 days on the MS medium and transferred to the same medium (+N) or to a nitrogen-deficient medium (-N) (left panel); or transferred to the same medium (-mannitol) or to same medium containing 300 mM mannitol (+mannitol) (right panel) for additional 4 days. The extracts were treated in the absence (un-Ex) or in the presence of 200  $\mu$ M  $\text{Na}_2\text{S}_4$  for 30 min ( $\text{Na}_2\text{S}_4$ -EX); CrATG8 was added to the incubation mixture and ATG4 activity monitored. Lane 1, processed pCrATG8 and lane 2, unprocessed CrATG8.

The ATG4 activity was monitored at the indicated times by immunoblotting analysis with anti-CrATG8. All procedures were performed at 25°C. Ponceau staining is shown as the protein loading control.

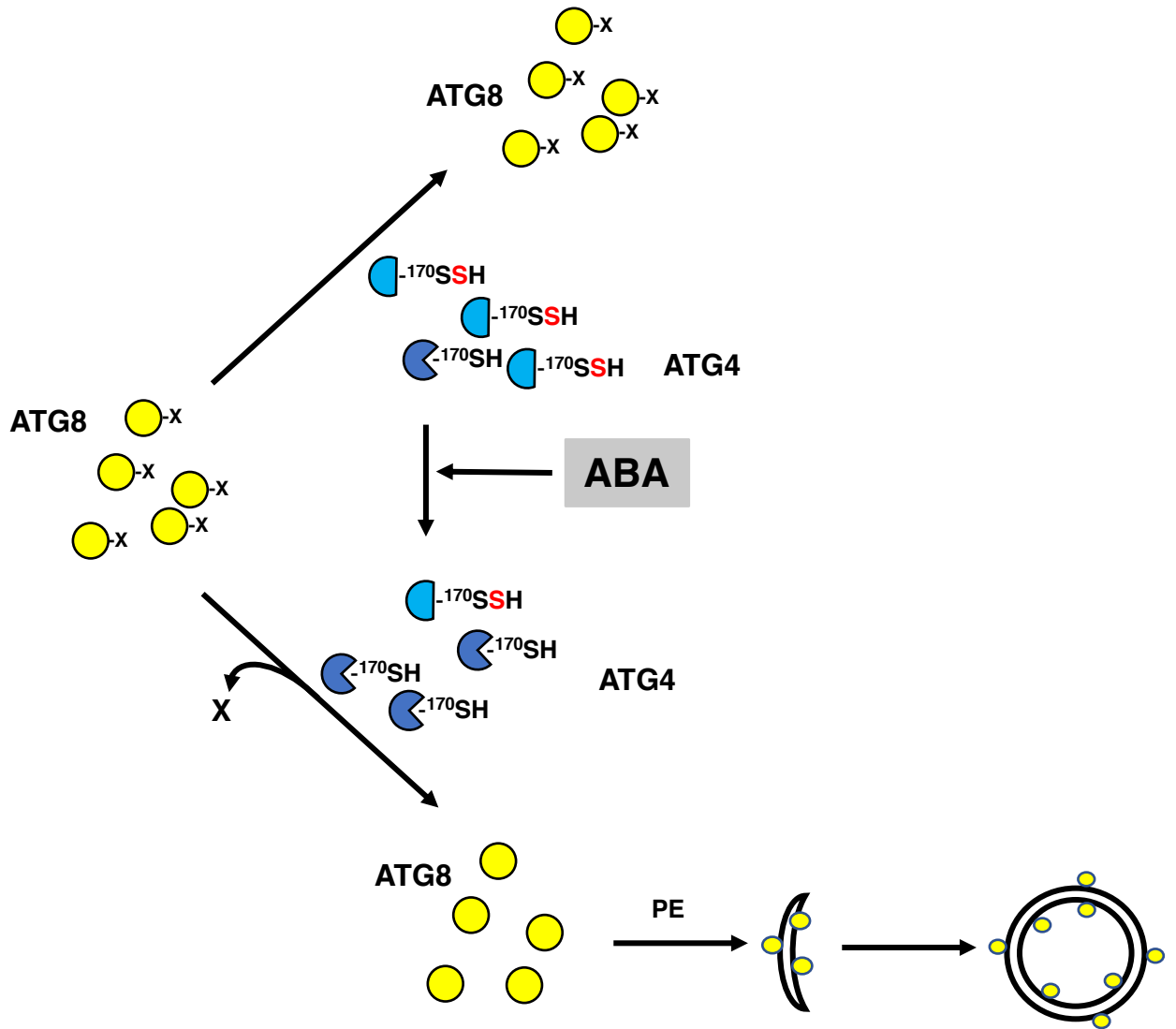


**Figure 10.** Graphical model of ABA-triggered autophagy induction through ATG4 posttranslational modification. Under basal conditions intracellular sulfide maintains high levels of persulfidation of the ATG4 pool which inhibits the proteolytic activity of the enzyme for ATG8 C-terminal processing. Increase in the intracellular level of ABA transiently decreases the level of persulfidation of the ATG4 population, activating the protease activity of the enzyme and the processing of ATG8 that can be further lipidated for the progression of autophagy. Yellow circles represent ATG8 protein with or without the C-terminal processed end (represented as X). Blue semicircles represent persulfidated ATG4 protein at the thiol  $^{170}$ Cys residue. Blue Pacman symbols represent ATG4 protein with reduced thiol  $^{170}$ Cys residue. The conjugation process of ATG8 with phosphatidylethanolamine (PE), autophagosome initiation and closure are also shown.



## IN A NUTSHELL

**Background:** Hydrogen sulfide ( $H_2S$ ) is a poisonous substance hazardous to life and the environment, but it is also present in biological tissues. Intense investigation showed that  $H_2S$  functions as an important regulator of essential processes in animals and plants. For example, our previous research on the plant *Arabidopsis* demonstrated that  $H_2S$  regulates autophagy. In autophagy (which is conserved in plants and animals), cell contents are digested for recycling. The materials to be digested are sequestered in a double membrane-bound structures called autophagosomes and the proteins involved in the main molecular machinery are referred to as autophagy-related (ATG). Autophagy is involved in plant development, immune responses, and adaptation to adverse environmental conditions.

**Question:** We wanted to know the mechanism of action by which  $H_2S$  regulates autophagy. Previous findings showed that  $H_2S$  is not a reductant in autophagy. We want to determine if the mechanism is persulfidation, a posttranslational protein modification of the thiol group of cysteines to form a persulfide group, and to identify the target ATG proteins.

**Findings:** Using proteomic analysis of *Arabidopsis* leaves treated with the hormone abscisic acid (ABA), we found that persulfidation of the cysteine protease ATG4 controls autophagy. When the persulfidation level of ATG4 is reduced after a short ABA treatment the autophagy progresses. This ATG4 protease undergoes specific persulfidation of the Cys170 residue that is a part of the catalytic site. ATG4 catalyzes the processing of newly synthesized ATG8, which is essential for the synthesis of autophagosomes. This activity was measured in a heterologous assay using *Chlamydomonas* ATG8 as substrate and we demonstrated that  $H_2S$  significantly and reversibly inactivates the proteolytic activity of ATG4. Under autophagy-inducing conditions such as nitrogen starvation and osmotic stress, we detected a significant increase in the overall ATG4 proteolytic activity that can be inhibited by sulfide.

**Next steps:** Our study demonstrated that negative regulation of autophagy by  $H_2S$  is mediated by persulfidation of ATG4. Probably this is not the only protein and additional targets remain to be identified. We will also investigate the role of  $H_2S$  in the regulation of selective autophagy and the interplay between  $H_2S$  and other regulators.



## Parsed Citations

- Alvarez C, Garcia I, Moreno I, Perez-Perez ME, Crespo JL, Romero LC, Gotor C (2012) Cysteine-generated sulfide in the cytosol negatively regulates autophagy and modulates the transcriptional profile in Arabidopsis. *Plant Cell* 24: 4621-4634.  
Google Scholar: [Author Only](#) [Title Only](#) [Author and Title](#)
- Aroca A, Gotor C, Romero LC (2018) Hydrogen Sulfide Signaling in Plants: Emerging Roles of Protein Persulfidation. *Front Plant Sci* 9.  
Google Scholar: [Author Only](#) [Title Only](#) [Author and Title](#)
- Aroca A, Benito JM, Gotor C, Romero LC (2017a) Persulfidation proteome reveals the regulation of protein function by hydrogen sulfide in diverse biological processes in Arabidopsis. *J Exp Bot* 68: 4915-4927.  
Google Scholar: [Author Only](#) [Title Only](#) [Author and Title](#)
- Aroca A, Schneider M, Scheibe R, Gotor C, Romero LC (2017b) Hydrogen Sulfide Regulates the Cytosolic/Nuclear Partitioning of Glyceraldehyde-3-Phosphate Dehydrogenase by Enhancing its Nuclear Localization. *Plant Cell Physiol* 58: 983-992.  
Google Scholar: [Author Only](#) [Title Only](#) [Author and Title](#)
- Aroca A, Serna A, Gotor C, Romero LC (2015) S-Sulfhydration: A Cysteine Posttranslational Modification in Plant Systems. *Plant Physiol* 168: 334-342.  
Google Scholar: [Author Only](#) [Title Only](#) [Author and Title](#)
- Calderwood A, Kopriva S (2014) Hydrogen sulfide in plants: From dissipation of excess sulfur to signaling molecule. *Nitric Oxide* 41C: 72-78.  
Google Scholar: [Author Only](#) [Title Only](#) [Author and Title](#)
- Chen S, Jia H, Wang X, Shi C, Wang X, Ma P, Wang J, Ren M, Li J (2020) Hydrogen Sulfide Positively Regulates Abscisic Acid Signaling through Persulfidation of SnRK2.6 in Guard Cells. *Mol Plant*.  
Google Scholar: [Author Only](#) [Title Only](#) [Author and Title](#)
- Chung T, Phillips AR, Vierstra RD (2010) ATG8 lipidation and ATG8-mediated autophagy in Arabidopsis require ATG12 expressed from the differentially controlled ATG12A AND ATG12B loci. *Plant J* 62: 483-493.  
Google Scholar: [Author Only](#) [Title Only](#) [Author and Title](#)
- Doelling JH, Walker JM, Friedman EM, Thompson AR, Vierstra RD (2002) The APG8/12-activating enzyme APG7 is required for proper nutrient recycling and senescence in Arabidopsis thaliana. *J Biol Chem* 277: 33105-33114.  
Google Scholar: [Author Only](#) [Title Only](#) [Author and Title](#)
- Doka E, Ida T, Dagnell M, Abiko Y, Luong NC, Balog N, Takata T, Espinosa B, Nishimura A, Cheng Q, Funato Y, Miki H, Fukuto JM, Prigge JR, Schmidt EE, Arner ESJ, Kumagai Y, Akaike T, Nagy P (2020) Control of protein function through oxidation and reduction of persulfidated states. *Sci Adv* 6: eaax8358.  
Google Scholar: [Author Only](#) [Title Only](#) [Author and Title](#)
- Dong Y, Silbermann M, Speiser A, Forieri I, Linster E, Poschet G, Allboje Samami A, Wanatabe M, Sticht C, Teleman AA, Deragon JM, Saito K, Hell R, Wirtz M (2017) Sulfur availability regulates plant growth via glucose-TOR signaling. *Nat Commun* 8: 1174.  
Google Scholar: [Author Only](#) [Title Only](#) [Author and Title](#)
- Garcia-Mata C, Lamattina L (2013) Gasotransmitters are emerging as new guard cell signaling molecules and regulators of leaf gas exchange. *Plant Sci* 201-202: 66-73.  
Google Scholar: [Author Only](#) [Title Only](#) [Author and Title](#)
- Gotor C, Garcia I, Crespo JL, Romero LC (2013) Sulfide as a signaling molecule in autophagy. *Autophagy* 9: 609-611.  
Google Scholar: [Author Only](#) [Title Only](#) [Author and Title](#)
- Gotor C, Laureano-Marin AM, Moreno I, Aroca A, Garcia I, Romero LC (2015) Signaling in the plant cytosol: cysteine or sulfide? *Amino Acids* 47: 2155-2164.  
Google Scholar: [Author Only](#) [Title Only](#) [Author and Title](#)
- Gotor C, Laureano-Marín AM, Arenas-Alfonseca L, Moreno I, Aroca A, García I, Romero LC. (2017). Advances in Plant Sulfur Metabolism and Signaling. In *Progress in Botany Vol. 78*, F.M. Cánovas, U. Lüttge, and R. Matyssek, eds (Cham: Springer International Publishing), pp. 45-66.  
Google Scholar: [Author Only](#) [Title Only](#) [Author and Title](#)
- Gotor C, Garcia I, Aroca A, Laureano-Marin AM, Arenas-Alfonseca L, Jurado-Flores A, Moreno I, Romero LC (2019) Signaling by hydrogen sulfide and cyanide through posttranslational modification. *J Exp Bot*.  
Google Scholar: [Author Only](#) [Title Only](#) [Author and Title](#)
- Gu L, Jung HJ, Kim BM, Xu T, Lee K, Kim YO, Kang H (2015) A chloroplast-localized S1 domain-containing protein SRRP1 plays a role in Arabidopsis seedling growth in the presence of ABA. *J Plant Physiol* 189: 34-41.  
Google Scholar: [Author Only](#) [Title Only](#) [Author and Title](#)
- Guiboileau A, Avila-Ospina L, Yoshimoto K, Soulay F, Azzopardi M, Marmagne A, Lothier J, Masclaux-Daubresse C (2013) Physiological and metabolic consequences of autophagy deficiency for the management of nitrogen and protein resources in Arabidopsis leaves depending on nitrate availability. *New Phytol* 199: 683-694.

Google Scholar: [Author Only](#) [Title Only](#) [Author and Title](#)

Hanaoka H, Noda T, Shirano Y, Kato T, Hayashi H, Shibata D, Tabata S, Ohsumi Y (2002) Leaf senescence and starvation-induced chlorosis are accelerated by the disruption of an Arabidopsis autophagy gene. *Plant Physiol* 129: 1181-1193.

Google Scholar: [Author Only](#) [Title Only](#) [Author and Title](#)

Ida T, Sawa T, Ihara H, Tsuchiya Y, Watanabe Y, Kumagai Y, Suematsu M, Motohashi H, Fujii S, Matsunaga T, Yamamoto M, Ono K, Devarie-Baez NO, Xian M, Fukuto JM, Akaike T (2014) Reactive cysteine persulfides and S-polythiolation regulate oxidative stress and redox signaling. *Proc Natl Acad Sci USA* 111: 7606-7611.

Google Scholar: [Author Only](#) [Title Only](#) [Author and Title](#)

Jin Z, Pei Y (2015) Physiological Implications of Hydrogen Sulfide in Plants: Pleasant Exploration behind Its Unpleasant Odour. *Oxid Med Cell Longev* 2015: 397502.

Google Scholar: [Author Only](#) [Title Only](#) [Author and Title](#)

Jin Z, Xue S, Luo Y, Tian B, Fang H, Li H, Pei Y (2013) Hydrogen sulfide interacting with abscisic acid in stomatal regulation responses to drought stress in Arabidopsis. *Plant Physiol Biochem* 62: 41-46.

Google Scholar: [Author Only](#) [Title Only](#) [Author and Title](#)

Kimura H (2015) Hydrogen sulfide and polysulfides as signaling molecules. *Proc Jpn Acad Ser B Phys Biol Sci* 91: 131-159.

Google Scholar: [Author Only](#) [Title Only](#) [Author and Title](#)

Kirisako T, Ichimura Y, Okada H, Kabeya Y, Mizushima N, Yoshimori T, Ohsumi M, Takao T, Noda T, Ohsumi Y (2000) The reversible modification regulates the membrane-binding state of Apg8/Aut7 essential for autophagy and the cytoplasm to vacuole targeting pathway. *J Cell Biol* 151: 263-276.

Google Scholar: [Author Only](#) [Title Only](#) [Author and Title](#)

Klie S, Nikoloski Z (2012) The Choice between MapMan and Gene Ontology for Automated Gene Function Prediction in Plant Science. *Front Genet* 3: 115.

Google Scholar: [Author Only](#) [Title Only](#) [Author and Title](#)

Laureano-Marin AM, Moreno I, Romero LC, Gotor C (2016a) Negative Regulation of Autophagy by Sulfide Is Independent of Reactive Oxygen Species. *Plant Physiol* 171: 1378-1391.

Google Scholar: [Author Only](#) [Title Only](#) [Author and Title](#)

Laureano-Marin AM, Moreno I, Aroca Á, García I, Romero LC, Gotor C. (2016b). Regulation of Autophagy by Hydrogen Sulfide. In *Gasotransmitters in Plants: The Rise of a New Paradigm in Cell Signaling*, L. Lamattina and C. García-Mata, eds (Cham: Springer International Publishing), pp. 53-75.

Google Scholar: [Author Only](#) [Title Only](#) [Author and Title](#)

Li Y, Zhang Y, Wang L, Wang P, Xue Y, Li X, Qiao X, Zhang X, Xu T, Liu G, Li P, Chen C (2017) Autophagy impairment mediated by S-nitrosation of ATG4B leads to neurotoxicity in response to hyperglycemia. *Autophagy* 13: 1145-1160.

Google Scholar: [Author Only](#) [Title Only](#) [Author and Title](#)

Liu Y, Bassham DC (2012) Autophagy: pathways for self-eating in plant cells. *Annu Rev Plant Biol* 63: 215-237.

Google Scholar: [Author Only](#) [Title Only](#) [Author and Title](#)

Liu Y, Xiong Y, Bassham DC (2009) Autophagy is required for tolerance of drought and salt stress in plants. *Autophagy* 5: 954-963.

Google Scholar: [Author Only](#) [Title Only](#) [Author and Title](#)

Marshall RS, Vierstra RD (2018a) Autophagy: The Master of Bulk and Selective Recycling. *Annu Rev Plant Biol*.

Google Scholar: [Author Only](#) [Title Only](#) [Author and Title](#)

Marshall RS, Vierstra RD (2018b) Autophagy: The Master of Bulk and Selective Recycling. *Annu Rev Plant Biol* 69: 173-208.

Google Scholar: [Author Only](#) [Title Only](#) [Author and Title](#)

Masclaux-Daubresse C, Chen Q, Have M (2017) Regulation of nutrient recycling via autophagy. *Curr Opin Plant Biol* 39: 8-17.

Google Scholar: [Author Only](#) [Title Only](#) [Author and Title](#)

Mishanina TV, Libiad M, Banerjee R (2015) Biogenesis of reactive sulfur species for signaling by hydrogen sulfide oxidation pathways. *Nat Chem Biol* 11: 457-464.

Google Scholar: [Author Only](#) [Title Only](#) [Author and Title](#)

Mizushima N, Yoshimori T, Ohsumi Y (2011) The role of Atg proteins in autophagosome formation. *Annu Rev Cell Dev Biol* 27: 107-132.

Google Scholar: [Author Only](#) [Title Only](#) [Author and Title](#)

Mustafa AK, Gadalla MM, Sen N, Kim S, Mu W, Gazi SK, Barrow RK, Yang G, Wang R, Snyder SH (2009) H<sub>2</sub>S signals through protein S-sulfhydration. *Sci Signal* 2: ra72.

Google Scholar: [Author Only](#) [Title Only](#) [Author and Title](#)

Nair U, Yen W-L, Mari M, Cao Y, Xie Z, Baba M, Reggiori F, Klionsky DJ (2012) A role for Atg8-PE deconjugation in autophagosome biogenesis. *Autophagy* 8: 780-793.

Google Scholar: [Author Only](#) [Title Only](#) [Author and Title](#)

Nakatogawa H, Ishii J, Asai E, Ohsumi Y (2012) Atg4 recycles inappropriately lipidated Atg8 to promote autophagosome biogenesis. *Autophagy* 8: 177-186.

Google Scholar: [Author Only](#) [Title Only](#) [Author and Title](#)

Papanatsiou M, Scuffi D, Blatt MR, García-Mata C (2015) Hydrogen Sulfide Regulates Inward-Rectifying K<sup>+</sup> Channels in Conjunction with Stomatal Closure. *Plant Physiol* 168: 29-35.

Google Scholar: [Author Only](#) [Title Only](#) [Author and Title](#)

Paul BD, Snyder SH (2012) H<sub>2</sub>S signalling through protein sulfhydration and beyond. *Nat Rev Mol Cell Biol* 13: 499-507.

Google Scholar: [Author Only](#) [Title Only](#) [Author and Title](#)

Perez-Perez ME, Florencio FJ, Crespo JL (2010) Inhibition of Target of Rapamycin Signaling and Stress Activate Autophagy in *Chlamydomonas reinhardtii*. *Plant Physiol* 152: 1874-1888.

Google Scholar: [Author Only](#) [Title Only](#) [Author and Title](#)

Perez-Perez ME, Lemaire SD, Crespo JL (2016) Control of Autophagy in *Chlamydomonas* Is Mediated through Redox-Dependent Inactivation of the ATG4 Protease. *Plant Physiol* 172: 2219-2234.

Google Scholar: [Author Only](#) [Title Only](#) [Author and Title](#)

Perez-Perez ME, Zaffagnini M, Marchand CH, Crespo JL, Lemaire SD (2014) The yeast autophagy protease Atg4 is regulated by thioredoxin. *Autophagy* 10: 1953-1964.

Google Scholar: [Author Only](#) [Title Only](#) [Author and Title](#)

Pérez-Pérez ME, Lemaire SD, Crespo JL (2012) Reactive oxygen species and autophagy in plants and algae. *Plant Physiol* 160: 156-164.

Google Scholar: [Author Only](#) [Title Only](#) [Author and Title](#)

Phillips AR, Suttangkakul A, Vierstra RD (2008) The ATG12-conjugating enzyme ATG10 Is essential for autophagic vesicle formation in *Arabidopsis thaliana*. *Genetics* 178: 1339-1353.

Google Scholar: [Author Only](#) [Title Only](#) [Author and Title](#)

Romero LC, Garcia I, Gotor C (2013) L-Cysteine Desulfhydrase 1 modulates the generation of the signaling molecule sulfide in plant cytosol. *Plant Signal Behav* 8: e24007.

Google Scholar: [Author Only](#) [Title Only](#) [Author and Title](#)

Sali A, Blundell TL (1993) Comparative protein modelling by satisfaction of spatial restraints. *J Mol Biol* 234: 779-815.

Google Scholar: [Author Only](#) [Title Only](#) [Author and Title](#)

Sato A, Sato Y, Fukao Y, Fujiwara M, Umezawa T, Shinozaki K, Hibi T, Taniguchi M, Miyake H, Goto DB, Uozumi N (2009) Threonine at position 306 of the KAT1 potassium channel is essential for channel activity and is a target site for ABA-activated SnRK2/OST1/SnRK2.6 protein kinase. *Biochem J* 424: 439-448.

Google Scholar: [Author Only](#) [Title Only](#) [Author and Title](#)

Satoo K, Noda NN, Kumeta H, Fujioka Y, Mizushima N, Ohsumi Y, Inagaki F (2009) The structure of Atg4B-LC3 complex reveals the mechanism of LC3 processing and delipidation during autophagy. *EMBO J* 28: 1341-1350.

Google Scholar: [Author Only](#) [Title Only](#) [Author and Title](#)

Scherz-Shouval R, Shvets E, Fass E, Shorer H, Gil L, Elazar Z (2007) Reactive oxygen species are essential for autophagy and specifically regulate the activity of Atg4. *EMBO J* 26: 1749-1760.

Google Scholar: [Author Only](#) [Title Only](#) [Author and Title](#)

Scuffi D, Álvarez C, Laspina N, Gotor C, Lamattina L, García-Mata C (2014) Hydrogen Sulfide Generated by L-Cysteine Desulfhydrase Acts Upstream of Nitric Oxide to Modulate Abscisic Acid-Dependent Stomatal Closure. *Plant Physiol* 166: 2065-2076.

Google Scholar: [Author Only](#) [Title Only](#) [Author and Title](#)

Scuffi D, Nietzel T, Di Fino LM, Meyer AJ, Lamattina L, Schwarzländer M, Laxalt AM, García-Mata C (2018) Hydrogen Sulfide Increases Production of NADPH Oxidase-Dependent Hydrogen Peroxide and Phospholipase D-Derived Phosphatidic Acid in Guard Cell Signaling. *Plant Physiol* 176: 2532.

Google Scholar: [Author Only](#) [Title Only](#) [Author and Title](#)

Sen N (2017) Functional and Molecular Insights of Hydrogen Sulfide Signaling and Protein Sulfhydration. *J Mol Biol* 429: 543-561.

Google Scholar: [Author Only](#) [Title Only](#) [Author and Title](#)

Seo E, Woo J, Park E, Bertolani SJ, Siegel JB, Choi D, Dinesh-Kumar SP (2016) Comparative analyses of ubiquitin-like ATG8 and cysteine protease ATG4 autophagy genes in the plant lineage and cross-kingdom processing of ATG8 by ATG4. *Autophagy* 12: 2054-2068.

Google Scholar: [Author Only](#) [Title Only](#) [Author and Title](#)

Shen J, Zhang J, Zhou M, Zhou H, Cui B, Gotor C, Romero LC, Fu L, Yang J, Foyer CH, Pan Q, Shen W, Xie Y (2020) Persulfidation-based Modification of Cysteine Desulfhydrase and the NADPH Oxidase RBOHD Controls Guard Cell Abscisic Acid Signaling. *Plant Cell* 32: 1000-1017.

Google Scholar: [Author Only](#) [Title Only](#) [Author and Title](#)

Shu CW, Drag M, Bekes M, Zhai D, Salvesen GS, Reed JC (2010) Synthetic substrates for measuring activity of autophagy proteases:

autophagins (Atg4). *Autophagy* 6: 936-947.

Google Scholar: [Author Only](#) [Title Only](#) [Author and Title](#)

Soto-Burgos J, Zhuang X, Jiang L, Bassham DC (2018) Dynamics of Autophagosome Formation. *Plant Physiol* 176: 219-229.

Google Scholar: [Author Only](#) [Title Only](#) [Author and Title](#)

Sugawara K, Suzuki NN, Fujioka Y, Mizushima N, Ohsumi Y, Inagaki F (2005) Structural basis for the specificity and catalysis of human Atg4B responsible for mammalian autophagy. *J Biol Chem* 280: 40058-40065.

Google Scholar: [Author Only](#) [Title Only](#) [Author and Title](#)

Thimm O, Blasing O, Gibon Y, Nagel A, Meyer S, Kruger P, Selbig J, Muller LA, Rhee SY, Stitt M (2004) MAPMAN: a user-driven tool to display genomics data sets onto diagrams of metabolic pathways and other biological processes. *Plant J* 37: 914-939.

Google Scholar: [Author Only](#) [Title Only](#) [Author and Title](#)

Toohey JI (2011) Sulfur signaling: is the agent sulfide or sulfane? *Anal Biochem* 413: 1-7.

Google Scholar: [Author Only](#) [Title Only](#) [Author and Title](#)

Ustun S, Hafren A, Hofius D (2017) Autophagy as a mediator of life and death in plants. *Curr Opin Plant Biol* 40: 122-130.

Google Scholar: [Author Only](#) [Title Only](#) [Author and Title](#)

Vanhee C, Batoko H (2011) Autophagy involvement in responses to abscisic acid by plant cells. *Autophagy* 7: 655-656.

Google Scholar: [Author Only](#) [Title Only](#) [Author and Title](#)

Vanhee C, Zapotoczny G, Masquelier D, Ghislain M, Batoko H (2011) The Arabidopsis Multistress Regulator TSPO Is a Heme Binding Membrane Protein and a Potential Scavenger of Porphyrins via an Autophagy-Dependent Degradation Mechanism. *The Plant Cell* 23: 785-805.

Google Scholar: [Author Only](#) [Title Only](#) [Author and Title](#)

Vitvitsky V, Miljkovic JL, Bostelaar T, Adhikari B, Yadav PK, Steiger AK, Torregrossa R, Pluth MD, Whiteman M, Banerjee R, Filipovic MR (2018) Cytochrome c Reduction by H<sub>2</sub>S Potentiates Sulfide Signaling. *ACS Chem Biol* 13: 2300-2307.

Google Scholar: [Author Only](#) [Title Only](#) [Author and Title](#)

Wang M, Tang W, Zhu YZ (2017) An Update on AMPK in Hydrogen Sulfide Pharmacology. *Front Pharmacol* 8: 810.

Google Scholar: [Author Only](#) [Title Only](#) [Author and Title](#)

Wang P, Zhao Y, Li Z, Hsu CC, Liu X, Fu L, Hou YJ, Du Y, Xie S, Zhang C, Gao J, Cao M, Huang X, Zhu Y, Tang K, Wang X, Tao WA, Xiong Y, Zhu JK (2018) Reciprocal Regulation of the TOR Kinase and ABA Receptor Balances Plant Growth and Stress Response. *Mol Cell* 69: 100-112 e106.

Google Scholar: [Author Only](#) [Title Only](#) [Author and Title](#)

Wedmann R, Onderka C, Wei S, Szijarto IA, Miljkovic JL, Mitrovic A, Lange M, Savitsky S, Yadav PK, Torregrossa R, Harrer EG, Harrer T, Ishii I, Gollasch M, Wood ME, Galardon E, Xian M, Whiteman M, Banerjee R, Filipovic MR (2016) Improved tag-switch method reveals that thioredoxin acts as depersulfidase and controls the intracellular levels of protein persulfidation. *Chem Sci* 7: 3414-3426.

Google Scholar: [Author Only](#) [Title Only](#) [Author and Title](#)

Woo J, Park E, Dinesh-Kumar SP (2014) Differential processing of Arabidopsis ubiquitin-like Atg8 autophagy proteins by Atg4 cysteine proteases. *Proc Natl Acad Sci U S A* 111: 863-868.

Google Scholar: [Author Only](#) [Title Only](#) [Author and Title](#)

Wu D, Wang H, Teng T, Duan S, Ji A, Li Y (2018) Hydrogen sulfide and autophagy: A double edged sword. *Pharmacol Res* 131: 120-127.

Google Scholar: [Author Only](#) [Title Only](#) [Author and Title](#)

Xiong Y, Contento AL, Bassham DC (2005) AtATG18a is required for the formation of autophagosomes during nutrient stress and senescence in Arabidopsis thaliana. *Plant J* 42: 535-546.

Google Scholar: [Author Only](#) [Title Only](#) [Author and Title](#)

Xiong Y, Contento AL, Nguyen PQ, Bassham DC (2007) Degradation of oxidized proteins by autophagy during oxidative stress in Arabidopsis. *Plant Physiol* 143: 291-299.

Google Scholar: [Author Only](#) [Title Only](#) [Author and Title](#)

Yoshimoto K, Hanaoka H, Sato S, Kato T, Tabata S, Noda T, Ohsumi Y (2004) Processing of ATG8s, ubiquitin-like proteins, and their deconjugation by ATG4s are essential for plant autophagy. *Plant Cell* 16: 2967-2983.

Google Scholar: [Author Only](#) [Title Only](#) [Author and Title](#)

Yu Z-Q, Ni T, Hong B, Wang H-Y, Jiang F-J, Zou S, Chen Y, Zheng X-L, Klionsky DJ, Liang Y (2012) Dual roles of Atg8-PE deconjugation by Atg4 in autophagy. *Autophagy* 8: 883-892.

Google Scholar: [Author Only](#) [Title Only](#) [Author and Title](#)

Zaffagnini M, Fermani S, Marchand CH, Costa A, Sparla F, Rouhier N, Geigenberger P, Lemaire SD, Trost P (2019) Redox Homeostasis in Photosynthetic Organisms: Novel and Established Thiol-Based Molecular Mechanisms. *Antioxid Redox Signal* 31: 155-210.

Google Scholar: [Author Only](#) [Title Only](#) [Author and Title](#)

Zheng X, Yang Z, Gu Q, Xia F, Fu Y, Liu P, Yin XM, Li M (2020) The protease activity of human ATG4B is regulated by reversible oxidative modification. *Autophagy*: 1-13.



**Abscisic Acid-Triggered Persulfidation of Cysteine Protease ATG4 Mediates Regulation of Autophagy by Sulfide**

Ana M. Laureano-Marín, Angeles Aroca, Maria Esther Perez-Perez, Inmaculada Yruela, Ana Jurado-Flores, Inmaculada Moreno, J L. Crespo, Luis C. Romero and Cecilia Gotor  
*Plant Cell*; originally published online October 9, 2020;  
DOI 10.1105/tpc.20.00766

This information is current as of October 9, 2020

<b>Permissions</b>	<a href="https://www.copyright.com/ccc/openurl.do?sid=pd_hw1532298X&amp;issn=1532298X&amp;WT.mc_id=pd_hw1532298X">https://www.copyright.com/ccc/openurl.do?sid=pd_hw1532298X&amp;issn=1532298X&amp;WT.mc_id=pd_hw1532298X</a>
<b>eTOCs</b>	Sign up for eTOCs at: <a href="http://www.plantcell.org/cgi/alerts/ctmain">http://www.plantcell.org/cgi/alerts/ctmain</a>
<b>CiteTrack Alerts</b>	Sign up for CiteTrack Alerts at: <a href="http://www.plantcell.org/cgi/alerts/ctmain">http://www.plantcell.org/cgi/alerts/ctmain</a>
<b>Subscription Information</b>	Subscription Information for <i>The Plant Cell</i> and <i>Plant Physiology</i> is available at: <a href="http://www.aspb.org/publications/subscriptions.cfm">http://www.aspb.org/publications/subscriptions.cfm</a>